

BayMeth: Improved DNA methylation quantification for affinity capture sequencing data using a flexible Bayesian approach

Andrea Riebler^{1,2,3,*}, Mirco Menigatti⁴, Jenny Z. Song⁵, Aaron L. Statham⁵, Clare Stirzaker^{5,6}, Nadiya Mahmud⁷, Charles A. Mein⁷, Susan J. Clark^{5,6}, Mark D. Robinson^{1,8,*}

¹Institute of Molecular Life Sciences, University of Zurich, Winterthurerstrasse 190, CH-8057 Zurich, Switzerland

²Institute of Social- and Preventive Medicine, University of Zurich, Hirschengraben 84, CH-8001 Zurich, Switzerland

³Department of Mathematical Sciences, Norwegian University of Science and Technology, N-7491 Trondheim, Norway

⁴Institute of Molecular Cancer Research, University of Zurich, Winterthurerstrasse 190, CH-8057 Zurich, Switzerland

⁵Epigenetics Laboratory, Cancer Research Program, Garvan Institute of Medical Research, Sydney 2010, New South Wales, Australia

⁶St Vincent's Clinical School, University of NSW, Sydney 2052, NSW, Australia

⁷Genome Centre, Barts and the London, Queen Mary, University of London, Charterhouse Square, London EC1M 6BQ, United Kingdom

⁸SIB Swiss Institute of Bioinformatics, University of Zurich, Zurich, Switzerland

Email: Andrea Riebler* - andrea.riebler@math.ntnu.no; Mirco Menigatti - menigatti@imcr.uzh.ch; Jenny Z. Song - j.song@garvan.org.au; Aaron L. Statham - a.statham@garvan.org.au; Clare Stirzaker - c.stirzaker@garvan.org.au; Nadiya Mahmud - n.mahmud@qmul.ac.uk; Charles A. Mein - c.a.mein@qmul.ac.uk; Susan J. Clark - s.clark@garvan.org.au; Mark D. Robinson* - mark.robinson@imls.uzh.ch;

*Corresponding author

Abstract

Background: DNA methylation (DNAm) is a critical component of the epigenetic regulatory machinery and aberrations in DNAm patterns occur in many diseases, such as cancer. Mapping and understanding DNAm profiles offers considerable promise for reversing the aberrant states. There are several approaches to analyze DNAm, which vary widely in cost, resolution and coverage. Affinity capture and high-throughput sequencing of methylated DNA (e.g. MeDIP-seq or MBD-seq) strike a good balance between the high cost of whole genome bisulphite sequencing (WGBS) and the low coverage of methylation arrays. However, existing methods cannot adequately differentiate between hypomethylation patterns and low capture efficiency and do not offer flexibility to integrate copy number variation (CNV). Furthermore, no uncertainty estimates are provided, which may prove useful for combining data from multiple protocols or propagating into downstream analysis.

Results: We propose an empirical Bayes framework that uses a fully methylated (i.e. Sssl treated) control sample to transform observed read densities into regional methylation estimates. In our model, inefficient capture can readily be distinguished from low methylation levels by means of larger posterior variances. Furthermore, we can integrate CNV by introducing a multiplicative offset into our Poisson model framework. Notably, our model offers analytic expressions for the mean and variance of the methylation level and thus is fast to compute. Our algorithm outperforms existing approaches in terms of bias, mean-squared error and coverage probabilities as illustrated on multiple reference datasets. Although our method provides advantages even without the Sssl-control, considerable improvement is achieved by its incorporation.

Conclusions: Our model not only improves on existing methods, but allows explicit modeling of CNV, context-specific prior information and offers a computationally-efficient analytic estimator. Our method can be applied to methylated DNA affinity enrichment assays (e.g MBD-seq, MeDIP-seq) and a software implementation is freely available in the Bioconductor `Repitools` package.

Keywords: affinity capture, analytical solution, copy number variation, DNA methylation, epigenetics, empirical Bayes, high-throughput sequencing, hypergeometric function, SssI treated DNA.

Background

DNA methylation (DNAm) is a critical component in the regulation of gene expression, is precisely controlled in development and is known to be aberrantly distributed in many diseases, such as cancer and diabetes [1,2]. In differentiated cells, DNAm occurs primarily in the CpG dinucleotide context. For CpG-island-associated promoters, increases in DNAm (i.e. hypermethylation) induce repression of transcription, while hypomethylated promoters are generally transcriptionally active. In cancer, tumor suppressor gene promoters are frequently hypermethylated, and therefore silenced, while hypomethylation can activate oncogenes, which collectively can drive disease progression [3,4]. The detection and profiling of such abnormalities across cell types and patient cohorts is of great medical relevance, to both our basic understanding of how the disease manifests but also for the opportunities of translating this knowledge to the clinic [5]. Epigenetic patterns can be used as diagnostic markers, predictors of response to chemotherapy and for understanding mechanisms of disease progression [6–9]. Acquired epigenetic changes

are potentially reversible, which provides important therapeutic opportunities; notably, the US Food and Drug Administration has approved at least four epigenetic drugs and others are in late-stage clinical trials [8].

Four classes of methods are available to profile DNAm genome-wide: chemical conversion, endonuclease digestion, direct sequencing and affinity enrichment; combinations of techniques are also in use (e.g. reduced representation bisulphite sequencing (RRBS) [10]). For recent reviews of the available platforms, see [11–13]. Treatment of DNA with sodium bisulphite (BS) is the gold standard, giving a single-base readout that preserves methylated cytosines while unmethylated cytosines are converted to uracil [14]. This approach can be coupled with high-throughput sequencing, e.g. whole genome bisulphite sequencing (WGBS), or a “genotyping” microarray (e.g. Illumina Human Methylation 450k array [15]). Because WGBS is genome-wide, it inefficiently reveals methylation status for low CpG-density regions [16] and is cost-limiting for larger cohorts; however, recent statistical frameworks allow trading coverage for replication [17] and sequencing targeted regions may be a plausible way to increase efficiency [18, 19]. Meanwhile, Illumina arrays cover less than 2% of genomic CpG sites and are only available for profiling human DNA, while enzymatic digestion approaches are limited by the location of specific sequences. There is considerable excitement surrounding third generation sequencing technologies that directly infer methylation status, but these are not yet readily available and generally offer lower throughput [20, 21]. An attractive alternative that provides a good tradeoff between cost and coverage, albeit at lower resolution, is affinity capture of methylated DNA in combination with high-throughput sequencing (e.g. MeDIP-seq [6, 22]). Using affinity capture with antibodies to 5-methylcytosine or methyl-CpG binding domain-based (MBDCap) proteins, subpopulations of methylated DNA are captured, prepared, sequenced and mapped to a reference genome (see Laird et al. [11]). Åberg et al. [23] studied the use of MBD-seq for methylome-wide association studies on 1500 case-control samples, and proved the potential of MBD-seq as a cost-effective tool in large-scale disease studies. A recent comparative study highlighted that affinity capture methods can uncover a significantly larger fraction of differentially methylated regions than the Illumina 450k array [24]. With appropriate normalization, the density of mapped reads can be transformed to a quantitative readout of the regional methylation level. However, the capability of these procedures to interrogate a given genomic region is largely related to CpG-density, which influences the efficiency of capture and can differ from protocol to protocol [16, 25, 26]. Thus, statistical approaches are needed. Several methods have been proposed to estimate DNAm from affinity-based DNAm data. For example, methyl binding domain (MBD)-isolated Genome Sequencing, a variant of MBD-seq, assumed a constant

rate of reads genome-wide and used a single threshold to binarize as methylated or not [27].

State-of-the-art methods, such as Batman [22] and MEDIPS [28], build a linear model relating read density and CpG-density, which is then used to normalize the observed read densities. For MeDIP-seq data, both algorithms showed similar estimation performance [28], while MEDIPS is considerably more time-efficient. Recently, a tool called BALM used deep sequencing of MBD-captured populations and a bi-asymmetric-Laplace model to provide CpG-specific methylation estimates [29]. All methods, however, suffer from the same limitations: i) low capture efficiency cannot easily be distinguished from low methylation level; ii) other factors that directly affect read density, such as copy number variation (CNV), are not easily taken into account. For CNV correction, a few possibilities have emerged, such as omitting known regions of amplification [6] or adjusting read densities manually [30]; or, iii) adjust using read density from an input sample [29]. Very recently, a method based on combining profiles from MeDIP/MBD-seq and methylation-sensitive restriction enzyme sequencing (MRE-seq) on the same samples with a computational approach using conditional random fields appears promising [31].

We present a novel empirical Bayes model called BayMeth, based on the Poisson distribution, that explicitly models (affinity capture) read densities of a fully methylated control (e.g. SssI-treated DNA) together with those from a sample of interest. Here, SssI data provide the model an awareness of where in the genome the assay can detect DNAm and the model allows integration of CNV and potentially other estimable factors that affect read density. Notably, we derive an analytic expression for the mean methylation level and also for the variance. Interval estimates, such as credible intervals, can be computed using numerical integration of the analytical posterior marginal distributions. Using MBD-seq on human lung fibroblast (IMR-90) DNA, where “true” methylation levels are available from WGBS, we show favorable performance against existing approaches in terms of bias, mean-squared error, Spearman correlation and coverage probabilities. Notably, we show that improved performance can even be observed when ignoring SssI-data. Model-based SssI correction, however, does not only lead to better performance, but allows, in addition, to compare more easily data originating from different capture platforms by propagating the platform-specific uncertainty. In an application to MBD-seq data on human prostate carcinoma (LNCaP) cells, we show that directly integrating CNV data provides additional performance gains. The performance on historical data, where no matched SssI sample is available, is demonstrated using data on embryonic stem cells, and colon tumor and normal samples presented in [32].

Results

BayMeth: A Bayesian framework for translating read densities into methylation levels

DNAme data is obtained by MBD-seq or a similar affinity enrichment assay. Let y_{iS} and y_{iC} denote the observed number of (uniquely) mapped reads for genomic regions $i = 1, \dots, n$ for the sample of interest and the SssI control, respectively. Throughout this paper, we use non-overlapping 100bp regions that have at least 75% mappable bases (see Methods). Let

$$y_{iS} | \mu_i, \lambda_i \sim \text{Poisson} \left(f \times \frac{\text{cn}_i}{\text{ccn}} \times \mu_i \times \lambda_i \right), \text{ and} \quad (1)$$

$$y_{iC} | \lambda_i \sim \text{Poisson}(\lambda_i), \quad (2)$$

with $\lambda_i > 0$, $0 < \mu_i < 1$. Here, λ_i denotes the region-specific read density at full methylation, μ_i the regional methylation level and $f > 0$ represents the (effective) relative sequencing depth between libraries (i.e. a normalization offset). An approximately linear relationship between the copy number state and MBD-seq read density was established [33]. Hence, if needed, we include a multiplicative offset $\frac{\text{cn}_i}{\text{ccn}}$ into our model formulation, where cn_i denotes the copy number state at region i and ccn is cell's most prominent CNV state (e.g. two in normal cells).

Closed-form posterior methylation quantities

In a Bayesian framework, prior distributions are assigned to all parameters. The methylation level (μ_i) has support from zero to one. Potential priors include mixtures of beta distributions or a Dirac-Beta-Dirac mixture. In the latter, a beta distribution is combined with point masses placed on zero and on one. The mixture weights can be either unknown or fixed. By default, BayMeth assumes a uniform prior distribution (i.e., a beta distribution with both parameters set to 1) for μ_i . For the region-specific density, we assume a gamma distribution, i.e. $\lambda_i \sim \text{Ga}(\alpha, \beta)$ using shape $\alpha > 0$ and rate $\beta > 0$ hyperparameters, which are determined in a CpG-dependent manner (see next Section). To make inferences for the regional methylation levels, μ_i , we integrate out λ_i from the joint posterior distribution:

$$\begin{aligned} \mathbf{p}(\mu_i | y_{i1}, y_{i2}) &= \int_0^\infty \mathbf{p}(\lambda_i, \mu_i | y_{i1}, y_{i2}) d\lambda_i \\ &= \int_0^\infty \frac{\mathbf{p}(y_{i1} | \lambda_i, \mu_i) \mathbf{p}(y_{i2} | \lambda_i) \mathbf{p}(\lambda_i) \mathbf{p}(\mu_i)}{\mathbf{p}(y_{i1}, y_{i2})} d\lambda_i. \end{aligned}$$

Notably, $\mathbf{p}(y_{i1}, y_{i2})$ can be calculated analytically [34], so that the marginal posterior distribution

$$\mathbf{p}(\mu_i | y_{i1}, y_{i2}) = \frac{\mu_i^{y_{i1}}}{W} \left(1 - \frac{E(1 - \mu_i)}{\beta + 1 + E} \right)^{-(\alpha + y_{i1} + y_{i2})}, \quad (3)$$

is given in closed form with $E = f \cdot \frac{cn_i}{ccn}$ and

$$W = \frac{1}{y_{i1} + 1} \times {}_2F_1 \left(y_{i1} + y_{i2} + \alpha, 1; y_{i1} + 2; \frac{E}{\beta + 1 + E} \right).$$

where ${}_2F_1()$ is the Gauss hypergeometric function [35, page 558]. The posterior mean and the variance are analytically available (see Additional file 1) and therefore efficient to compute; credible intervals (quantile-based or HPD) can be computed from Equation (3). Wald credible intervals are computed on the logit scale, where $\text{logit}(\mu_i) = \log(\mu_i/(1 - \mu_i))$, and then transformed back. These intervals are based on assuming asymptotic normality of the logit methylation estimate. The 95% Wald interval on logit scale is computed by $\text{logit}(\hat{\mu}_i) \pm 1.96 \cdot \hat{\sigma}_i$, where $\hat{\sigma}_i$ is the standard error estimate of $\text{logit}(\hat{\mu}_i)$. For detailed statistical derivations, also including more general prior distributions for μ_i , we refer to the Additional file 1.

Empirical Bayes for prior hyperparameter specification

Our method takes advantage of the relationship between CpG-density and read depth to formulate a CpG-density-dependent prior distribution for λ_i (and possibly unknown parameters in the prior distribution of μ_i). Taking CpG-density into account the prior should stabilize the methylation estimation procedure for low counts and in the presence of sampling variability. All unknown hyperparameters are determined in a CpG-density-dependent manner using empirical Bayes. For each genomic bin of predetermined size, e.g., 100bp, we determine the weighted number of CpG dinucleotides within an enlarged window, say 700bp, around the center of the bin (see Methods and MEDME [36]). Each region is classified based on its CpG-density into one of $K(= 100)$ non-overlapping CpG-density intervals (see x-axis tick marks in Figure S1 of Additional file 2).

For each class separately, we derive the values for the hyperparameters under an empirical Bayes framework using maximum likelihood. Both read depths, from the SssI control and the sample of interest, are thereby taken into account, since λ_i is a joint parameter affecting both. We end up with K parameter sets. To illustrate the (known) relationship between SssI read count and CpG density, we considered only the SssI Poisson model (Equation (2)) and derived the prior predictive distribution by integrating λ_i out; this results in a negative binomial distribution for each CpG class (see Figure 1 using SssI data from [37] which are later used in the analysis of the IMR-90 cell line).

Sssl-free BayMeth

Although we recommend collecting at least a Sssl sample under the same protocol as the data of interest, BayMeth can, in principle, be run without a Sssl-control sample. The statistical framework then only involves the Poisson model for the sample of interest (Equation (1)) and no longer borrows strength from the information included in the Sssl-control sample (Equation (2)). The same model is used in the analysis of underreported count data in economics [34,38,39], where it is assumed that the number of registered purchase events underreports the actual purchase rate. According to Fader and Hardie [34] the parameters λ_i and μ_i are identifiable assuming that the gamma and beta prior distributions are able to capture unobserved heterogeneity in the read density rate and the methylation level. As in the framework with Sssl data, parameters for the gamma prior distributions of the region-specific read density λ can still be determined in dependence on the CpG density, however, no information can be borrowed from the fully methylated control. Furthermore, the determination of the normalizing offset f gets more involved. Interpretation moves from the (effective) relative sequencing depth between libraries to the number of bins potentially “under risk” to be methylated in the sample of interest. Here, we fix f at the 99th quantile of the number of reads. The results for the posterior mean and variance of the methylation level change accordingly (see Additional file 1).

Analysis of affinity capture methylation data with a matched Sssl sample

In the following, we apply BayMeth to affinity capture methylation data where we collected a Sssl-control sample under the same conditions (e.g. same elution protocol) used for the samples of interest. Hence, both data components are matched.

BayMeth improves estimation and provides realistic variability estimates

To take advantage of the Lister et al. [40] single-base-resolution high-coverage methylome obtained by WGBS, we generated IMR-90 MBD-seq data under the same protocol as our previously published Sssl MBD-seq dataset [37] i.e. using a single fraction with high salt elution buffer (MethylMinerTM). We applied BayMeth to chromosome 7 consisting of 1 588 214 non-overlapping bins of width 100bp. Only bins with at least 75% mappable bases were included, which leads to the analysis of 1 221 753 ($\sim 77\%$) bins. We run BayMeth in two configurations: 1) incorporating Sssl information and assuming a uniform prior between zero and one for the methylation parameter; 2) ignoring Sssl information and assuming a Dirac-Beta-Dirac mixture prior distribution for the methylation parameter. That means we set a point

mass on zero and on one, giving each a prior weight of 10%. The parameters of the central beta component are thereby assumed to be unknown. The normalizing offset $f = 0.581$ for configuration 1) is found based on calculating a scaling factor between highly methylated regions in IMR-90 relative to the SssI control (see Methods and Figure S2 of Additional file 2). The prior parameters for the gamma distributions, and the parameters of the beta distribution in configuration 2), are determined by empirical Bayes, as discussed above (see also further details in Methods). We compared the results of BayMeth, both ignoring and taking advantage of the SssI control, to those obtained by Batman [22], MEDIPS [28] and BALM [29]. To provide plausible uncertainty estimates with Batman, we increased the default number of generated samples from 100 to 500. The WGBS data, here considered to be the “truth” (at suitable depth), and the CpG-specific BALM methylation estimates are collapsed into 100bp bin estimates (see Methods) to match the estimates from MEDIPS, Batman and our approach. For about 53% (645 451) of the analyzed bins, no WGBS data are available (largely due to lack of CpG sites). For 17259 bins, no methylation estimates are provided by Batman, so that in total, algorithm comparisons are conducted on the remaining 559043 bins. The behavior of BayMeth (including SssI-information) and Batman is illustrated using an example region of chromosome 7 (see Figure 2A). WGBS levels, CpG-density and read counts per 100bp region of MBD-seq SssI and IMR-90 sample are shown. As expected, the number of reads in the SssI control is related to the CpG-density, whereas the read density in (MBD-seq) IMR-90 is modulated by both the region-specific density and the DNAm level. Regions lacking both IMR-90 and SssI reads suggest inefficient MBD-based affinity capture (e.g. region ‘a’). Figure 2B shows posterior samples from Batman and inferred posterior distributions from BayMeth. For region ‘a’, Batman’s posterior samples are concentrated between 0.7 and 1 (mean equal to 0.85). In contrast, BayMeth returns a mean methylation level of 0.49 together with a large 95% highest posterior density (HPD) interval (0, 0.94), reflecting the uncertainty from having no SssI reads sampled. The credible interval covers nearly the entire interval, reflecting that no reliable estimate can be made for this bin due to inefficient capture. For regions with no IMR-90 reads but efficient capture (e.g. region ‘b’), both BayMeth and Batman provide sensible posterior marginal distributions and low DNAm estimates. If there are a small number of reads for IMR-90 with efficient capture (e.g. region ‘c’), the BayMeth posterior marginal is more disperse than Batman’s, while both are close to zero. Region ‘d’ has a high number of reads for both samples and a true methylation level around 0.95. This level is covered by the 95% HPD region of BayMeth, while it lies outside of the density mass obtained by Batman overestimating this region.

Table 1 summarizes the estimation performance for chromosome 7 by means of mean bias (difference

between the posterior mean $\hat{\mu}_i$ and the true value μ_i), MSE (mean of squared differences), Spearman correlation and compares it to a BayMeth version ignoring SssI-information, Batman, MEDIPS and BALM. To account for uncertainty present in the WGBS estimates, we applied a threshold on the depth; we assess the performance using bins with at least 33 WGBS reads (unmethylated and methylated) corresponding to the 25% quantile of depth in the truth, which results in 414352 bins. Results are stratified into five groups according to depth in the SssI control, which should represent a surrogate of the capture efficiency. The first group $[0, 4]$ encompasses primarily low-CpG regions that are not well captured in MBD experiments, while the high $(27, 168]$ group represents primarily CpG island regions. On average, Batman tends to overestimate DNAm while MEDIPS and BALM tend to underestimate. BayMeth, in contrast, is almost unbiased. The smaller bias in the point estimates obtained by BayMeth is also reflected in the MSE. For all methods, the MSE decreases with higher SssI depth, as expected due to the efficiency of capture. For all depth groups, BayMeth has the highest correlation with the WGBS estimates, which increases with higher SssI depth. The SssI-free version of BayMeth performs comparable to the other approaches, with slightly smaller bias and MSE, however, smaller correlation for bins with low SssI depth. A smoothed density representation of regional methylation estimates for the highest SssI depth group, namely $(27, 168]$, plotted for all methods against the “true” WGBS methylation levels are shown in Figure 3; overall, BayMeth provides the most accurate point estimates. The overestimation of Batman and underestimation of MEDIPS and BALM is obvious, while the BayMeth errors vary almost symmetrically. Comparing BALM CpG-wise to WGBS lead to similar conclusions as in the bin-specific setting (results not shown). Notably, the pattern of the SssI-free BayMeth estimation (i.e. overestimation) is similar to Batman, which may be expected given that no information is drawn from the SssI sample.

To assess calibration, we computed coverage probabilities (frequency that the “true” methylation value is captured within a credible interval). Stratified by the “true” WGBS methylation level, Figure 4 shows coverage probabilities at 95% level for regions deemed to be inside or outside a CpG island (Figure S1 of Additional file 2). HPD intervals, quantile-based and Wald-based credible intervals (CI) are computed for BayMeth while only quantile-based CIs are available for Batman; coverage probabilities are not possible from MEDIPS and BALM output. As mentioned, Batman tends to underestimate the variance, resulting in lower coverage probabilities of the WGBS values; in contrast, BayMeth’s coverage probabilities are much closer to the nominal levels and seem to be stable across the stratification. For the SssI-free BayMeth quantile-based credible intervals are computed which are generally better than those provided by Batman (see Table 1 and Figure 4), indicating a more realistic methylation estimation. Table S1 in Additional

file 2) shows for the same stratification the mean bias for BayMeth, Batman, MEDIPS and BALM. While the latter two provide low mean bias for bins where the truth lies within $[0, 0.2]$, Batman performs best for highly methylated bins. BayMeth shows good performance for bins where the true methylation level is intermediate or high. Similar to Batman reasonable estimates are obtained over the whole range of methylation states when considering bins in CpG islands. Interpreting the mean bias the uncertainty around the obtained estimates should taken into account and hence the results should be set into context with Figure 4. Combining bias and calibration BayMeth shows good performance and seems to improve on existing approaches.

CNV-aware BayMeth improves DNAm estimation for prostate cancer cells

In the following, we illustrate the benefits of directly integrating CNV information into a cancer MBD-seq dataset. We apply our methodology to the autosomes of the LNCaP cell line. To motivate such an adjustment, Figure 5 shows the estimated copy number across chromosome 13 (with many non-neutral regions), together with tiled MBD-seq read counts. Copy number estimates were derived using the PICNIC algorithm on Affymetrix genotyping arrays (see Methods). Although read densities at a specific genomic region (again, 100bp non-overlapping bins) are influenced by a combination of effects (e.g. DNAm, CpG-density), a relationship between CNV and number of reads is clearly visible. In particular, a difference in read counts between regions with four copies and those with smaller copy numbers is apparent. We adjust for this bias through a multiplicative offset $\frac{cn_i}{ccn}$, where the prominent state is four copies, i.e., $ccn = 4$ in Equation (1) (see Figure S3 of Additional file 2); note, this also assumes the SssI sample originates for a “normal” copy genome. In addition, regions from this state ($cn_i = 4$) are used to determine the normalizing offset f (here, estimated to be 0.712). The read depth stratified by copy number state together with mean and median estimates is shown in Figure S4 of Additional file 2. In particular, for the three most frequent CNV states (2–4), read densities scale approximately linearly (with a slope of 1) with CNV, which justifies the structure of our multiplicative offset; copy-number offsets are given in Table 2. Figure 6 shows the bias of DNAm point estimates of the different methods by integer CNV state (2–5); here, we used the Illumina Human Methylation 450k array as the “true” methylation (see Methods), since methylation status should be unaffected by CNV [41]. Because CNV only affects MBD capture for methylated regions, we restrict this comparison to bins where the true methylation state is larger than 0.5 and we applied a threshold of 13 (median after excluding bins with a low depth of $[0, 4]$) to the number of reads in the SssI-control to select for regions where MBD-seq has good performance. Similar to the IMR-90

data, MEDIPS and BALM tend to underestimate, while Batman tends to overestimate. For BayMeth we show four different approaches neglecting CNV and/or SssI-information. As previously, we use a uniform prior for the methylation level when taking advantage of the SssI sample, and a Dirac-Beta-Dirac mixture with fixed weights (0.1, 0.8, 0.1) but unknown beta parameters in the SssI-free case. In the SssI-free version the normalization offset f is determined as the 99% percentile of the number of reads for the sample of interest having copy number state 4, while the reads of all bins are used when neglecting additionally the CNV information. Without the additional multiplicative offset (i.e. without $cn_i \equiv ccn$) to account for CNV, BayMeth provides biased estimates, predictably by CNV state. After including the copy-number-specific offset, these copy number specific biases almost disappear, whereby the SssI-free version still shows slight overestimation. A smoothed scatterplot illustrating the benefits of including the copy-number-specific offset is shown in Figure 7 for copy number state two. In particular, bins that have been falsely underestimated (due to two copies instead of four) are corrected (see top-right panel). Due to overestimation in the SssI-free version (bottom-left) the methylation estimates for copy number state two do not show such a strong bias. Adjusting for CNV in this case slightly increases the bias (bottom-right). Table 3 shows mean bias, MSE and Spearman correlation for the different approaches stratified by copy number state. In all measures, the CNV-aware standard (including SssI) version of BayMeth performs best. While the differences in the correlation estimates are small, clear advantages can be seen in terms of bias and MSE when compared to Batman, MEDIPS or BALM. In contrast to the other approaches, the bias/MSE performance estimates stay almost constant over the different copy number states and are close to zero.

Improved correlation across methylation kits on IMR-90 DNA

One potential advantage of the proposed model-based SssI correction is that data originating from different capture platforms can be more easily compared. In this situation, propagation of the uncertainty becomes important, since methods to capture methylated DNA have different CpG-dependent affinity and therefore different estimation precision. To demonstrate this, we captured methylated DNA from IMR-90 and SssI DNA using six approaches: low, medium and high salt elutions from MethylCap KitTM, 500nM and 1000nM salt fractions from MethylMinerTM and MeDIP. Autosomes were analyzed with BayMeth using specific SssI data for each kit. The derived MA-plots together with the obtained normalizing offsets f for each sample are shown in Figure S5 of Additional file 2. Unusual high counts were excluded in the derivation of the prior parameters [42], but methylation estimates are derived for all bins. For bins where

the estimated credible interval width (HPD) is smaller than 0.4, Figure 8 compares the unnormalized read density between the six kits (upper triangular panel), and the obtained methylation estimates (lower triangular panels). Clearly, capture affinities across the six kits vary drastically, while the SssI-based correction makes the comparison much clearer. In addition, the SssI data from this collection of platforms may be useful for the community to pair with their in-house data, assuming similar procedures have been followed (see Discussion), in order to benefit from the use of SssI-based read density correction from BayMeth.

Analysis of affinity capture methylation data WITHOUT a matched SssI sample

Next, we applied (default) BayMeth to the MethyCap sequencing data of [32], provided at <http://www.broadinstitute.org/labs/meissner/mirror/papers/meth-benchmark/index.html>, and denoted as the “Bock” data below. Absolute read densities are available for four samples: HUES6 ES cell line, HUES8 ES cell line, colon tumor tissue, colon normal tissue (same donor as for colon tumor tissue), and given for (non-overlapping) 50bp bins. There is no matched SssI sample available for these data. To take advantage of BayMeth in analyzing these data, we use a non-matching SssI sample, but one chosen to be maximally compatible to the preparation conditions of Bock data [32] (i.e. MethyCap at low salt concentration: 200mM NaCl). Regions from the data available were lifted over to hg19 coordinates (see Additional file 3 for details). Although there are still slight differences in the preparation of the samples of interest and the SssI sample, which arise from different used read length (36bp versus 75bp, respectively) and different read extensions (300bp versus 150bp, respectively) before calculating the read frequencies, we regard the SssI sample as a reasonably suitable control for running BayMeth. We analyzed all autosomes after removing bins that have no read depth in any of the four samples, leading to 42 955 764 bins. As in the previous analyses, we restrict our focus on bins that have at least 75% mappable bases, which means 37013409. That is 86% of all bins. A detailed description of all data preparation steps and the data analysis using BayMeth based on the R-package `Repitools` is given in Additional file 3. To assess the methylation estimates obtained with BayMeth, we compare them to RRBS data available from the Bock study [32]. As in the methylation kit analysis we masked unusual high counts in the derivation of the prior parameters as they sometimes cause problems in the numerical optimization routine, however, methylation estimates are derived for more than 99.5% of these masked bins. Interestingly, several high count regions are explained by unannotated high copy number regions, see Pickrell et al. [42].

Methylation estimates are obtained for about 37 million bins each of width 50bp, while RRBS estimates

are only available for approximately 4% of these bins. We assess the performance of BayMeth using bins where the depth in the RRBS is larger than 20. Furthermore, we focus on bins where we believe in the SssI control, that means where the read depth is at least 10. Figure 9 shows regional methylation estimates obtained by BayMeth compared to RRBS derived methylation levels for all four samples of interest where the corresponding posterior standard deviation is smaller than 0.15. In particular, low methylation levels are well predicted for all samples. While high methylation levels are partly underestimated by BayMeth for the human embryonic stem cell line HUES8, estimates for HUES 6, colon tumor and color normal tissue reproduce the true methylation for all levels. Although, in the latter two slight overestimation is visible. This is partly caused by bins for which we observe low read depth in SssI, but extreme depth in the sample of interest. BayMeth predicts these bins comprehensibly with high precision (low standard deviation), which may, however, not coincide with the RRBS estimates. Figure 10 shows regional posterior variances obtained by BayMeth compared to SssI depth for bins where the depth in the RRBS is larger than 20. The posterior variance decreases with increasing SssI depth. However, the range of posterior variances for low SssI depth is large. The red square contains the bins illustrated in Figure 9. Of note, comparisons to other methods are not possible for the Bock data, since we do not have access to the raw reads.

Discussion and conclusions

DNA methylation plays a crucial role in various biological processes and is known to be aberrant in several human diseases, such as cancer. There are now a multitude of methylation profiling platforms, each with inherent advantages and disadvantages. Bisulfite-based approaches are considered the gold standard since they allow quantification at single-base resolution. However, applied genome-wide, this technique can be inefficient and expensive, in terms of CpGs covered per read or base sequenced [5, 16]. On the other hand, affinity capture based approaches, such as MBD or MeDIP, combined with sequencing seem to provide a good compromise between cost and coverage, albeit at lower resolution. Thus, we consider MBD-seq and its variants to be an attractive alternative and have developed an efficient data analytic approach to facilitate their use. In addition, MBD-seq has recently been demonstrated using only hundreds of nanograms of starting DNA, thus making it applicable to a wider range of studies, such as clinical samples [43].

The key to our proposed method is the use of methylated DNA captured from a fully methylated SssI control; to facilitate accurate transformation of read counts into methylation, we recommend such a sample should be collected under the same conditions (e.g. same elution) used for the samples of interest. In our analyses, we used commercially available SssI-treated DNA [26, 37] for the MBD-seq experiments and

verified with the 450k platform that the overwhelming majority of CpG sites are indeed methylated (see Figure S6 of Additional file 2); similarly, such a sample can be constructed directly and inexpensively [44]. Our proposed method, BayMeth, is a flexible empirical Bayes approach that transforms read densities into regional methylation estimates. Our model is based on a Poisson distribution and takes advantage of SssI control data in two ways: i) we model SssI data jointly with data from a sample of interest to preserve the linearity of the methylation estimation; ii) we explicitly get information about the region-specific read density as a function of CpG-density. Our method is similar in principle to MEDME, which was applied to fully methylated MeDIP microarray intensities [36]. However, our approach necessarily modifies assumptions for count data (i.e. read densities versus probe intensities) and is effectively a *moderation* between the global fit that MEDME implements and a region-specific correction. We showed that BayMeth delivers improved performance against state-of-the-art techniques for MBD-seq data, using multiple datasets where independent “true” methylation levels are available from WGBS or bisulphite-based methylation arrays. In general, MEDIPS and BALM underestimate the methylation levels and do not offer variability estimates. Batman performs reasonably well, but our results suggest that variability estimates are generally underestimated and the method is very computationally demanding. Our model performs best in point estimation and is the only method that provides reasonable interval estimates. Notably, BayMeth offers analytic expressions for the posterior marginal distribution and the posterior mean and variance, avoiding computationally-expensive sampling algorithms. Furthermore, we can explicitly integrate existing CNV data, which offers improvement when applied to cancer datasets. CNV adjustments may be possible with existing approaches such as Batman or MEDIPS, based on ad-hoc transformations of the read counts (e.g. see [30]), but are not included within the model formulation. In contrast, our model preserves the count nature of the data. To adjust the modeled mean for effects arising due to library composition or CNV, we introduced a normalization offset. This strategy is quite general and could be extended beyond composition and CNV (e.g. see [33,45]).

A conceptual similar Bayesian hierarchical model, which involves MCMC sampling, has been proposed in the context of Methyl-Seq experiments, where methylation levels are derived based on enzymatic digestion using two enzymes [46]; a separate Poisson model is assumed for the tag counts of each enzyme. The models are linked through a shared parameter while one Poisson model contains a methylation level parameter μ , assumed to be uniformly distributed *a priori*; our model may have applications in this domain. In the applications presented here, a uniform prior distribution for the methylation level was observed to perform best when taking SssI information into account, while a mixture prior of a point mass

at zero and at one, combined with a beta distribution, performed best when ignoring SssI information. The analytical expressions for the mean, variance and posterior marginal distribution are also available when using a mixture of beta distributions (see Methods). Therefore, context-specific information, such as CpG-density or the position relative to transcriptional features, could be incorporated in the prior distribution for the methylation level. We have tried various weighted mixtures of two or three beta distributions that build in contextual information; however, these did not outperform the uniform prior when borrowing strength from the SssI sample. The reason lies probably in the fact that there is only one data point for each methylation parameter. Hence, using an informative prior distribution for the methylation level, it is very difficult for the data to overcome this prior guess.

It is well known that methylation levels are dependent within neighboring regions. Thus, a potential improvement may involve modeling correlation between neighboring genomic bins. One approach might be Gaussian Markov random fields [47]; however, the analytical summaries are lost, so the the gain in performance may not justify the more complex model and associated computational cost.

BayMeth may also be regarded as pre-processing step for performing differential methylation analysis. The uncertainty in methylation estimates obtained by BayMeth could be propagated to downstream analysis, which may lead to improved inference on differential methylation.

Methods

MBD-seq on IMR-90, LNCaP and SssI DNA

We used LNCaP and SssI MBD-seq data and Affymetrix genotyping array data (LNCaP only) from Robinson et al. [37]. The data can be found at <http://www.ncbi.nlm.nih.gov/geo> under accession number GSE24546. Similarly, IMR-90 MBD-seq is available from GSE38679. Details of the DNA capture, preparation and sequencing can be found in Robinson et al. [26,37].

MBD-seq and Methylated DNA Immunoprecipitation sequencing (MeDIP-seq) for comparing data from different methylation kits

For comparing data obtained by different methylation kits we captured methylated DNA from IMR-90 and SssI DNA as follows. Genomic DNA was sheared to 150-200bp using the Covaris S220 sonicator. MBD capture was performed using the MethylMiner Methylated DNA Enrichment Kit (Invitrogen) and the MethylCap Kit (Diagenode) following the manufactures recommended protocols. The bound fractions were eluted at 500mM and 1M NaCl for MethylMiner and with buffers at different salt concentrations (low, medium, high) for the MethylCap. Sequencing libraries were prepared with the SOLiD Fragment Library

Construction Kit (Applied Biosystems) MeDIP-seq methylation immunocapture and library preparation were performed using the MeDIP Kit (Active Motif) following the manufactures recommended protocol.

Calculation of CpG-density

CpG-density is defined to be a weighted count of CpG sites in a predefined region. We used the function `cpgDensityCalc` provided by the R-package `Repitools` [48] to get bin-specific CpG-density estimates using a linear weighting function and a window size of 700bp (since we expect fragments around 300bp).

Calculation of mappability

Using Bowtie, all possible 36bp reads of the genome were mapped back against the hg18 reference, with no mismatches. At each base, a read can either unambiguously map or not. A mappability estimate gives the proportion of reads that can be mapped to a specific regions. To get bin-specific mappability estimates we used the function `mappabilityCalc` in the `Repitools` package [48]. In our analysis, a window of 500bp was used (250bp upstream and downstream from the center from each 100bp bin) and the percentage of mappable bases was computed.

For the methylation kits analysis we used mappability estimates for hg19 provided by ENCODE on <http://hgdownload.cse.ucsc.edu/goldenPath/hg19/encodeDCC/wgEncodeMapability/wgEncodeCrgMapabilityAlign100mer.bigWig>, from which we derived a weighted mean based on the window size. Analogously, we used <http://hgdownload.cse.ucsc.edu/goldenPath/hg19/encodeDCC/wgEncodeMapability/wgEncodeCrgMapabilityAlign50mer.bigWig> for the Bock data analysis.

Derivation of region-specific methylation estimates from WGBS

In the Lister et al. IMR-90 WGBS data, the number of reads r_j^+ and r_j^- overlaying a cytosine j in the positive (+) and negative strand (-), respectively, is available. Furthermore, the number of these reads, m_j^+ and m_j^- , that contain a methylated cytosine, is known. A single-base methylation estimate can be obtained by $(m_j^+ + m_j^-)/(r_j^+ + r_j^-)$. To get a bin-specific methylation estimate all cytosines lying within a bin of interest \mathcal{B} are taken into account:

$$\mu_{\mathcal{B}} = \frac{\sum_{j \in \mathcal{B}} (m_j^+ + m_j^-)}{\sum_{j \in \mathcal{B}} (r_j^+ + r_j^-)}.$$

Here, $\sum_{j \in \mathcal{B}} (r_j^+ + r_j^-)$ is termed depth.

Derivation of region-specific methylation estimates from 450K arrays

First, the Illumina HumanMethylation450 methylation array was preprocessed using default parameter of the `minfi` package [49]; for each sample, a vector of *beta values*, one for each targeted CpG site representing methylation estimates are produced. To obtain (100bp) bin-specific methylation profiles, we averaged beta values from all CpG sites within 100bp (upstream and downstream; total window of 200bp) from the center of our 100bp bins.

Derivation of region-specific methylation estimates from RRBS data

For the Bock data analysis, information on RRBS data were available from <http://www.broadinstitute.org/labs/meissner/mirror/papers/meth-benchmark/index.html>, which we considered as gold standard. Both, the number of reads that overlay a cytosine (T) and the number of cytosines that stay a cytosine (M), i.e. are methylated, are given. Note, that for one CpG site there is only information from one strand available. To get smooth methylation estimates, we used 150bp bins (overlapping by 100bp). The methylation level for one 150bp bin i was derived as:

$$m_i = \frac{\sum M_{\in i}}{\sum T_{\in i}}.$$

That means using information for all CpG sites that fall into bin i .

Determining the normalizing offset

The composition of a library influences the resulting read densities [50]. For example, the SssI control represents a more diverse set of DNA fragments since it captures the vast majority of CpG rich regions in the genome. Therefore, if the total sequencing depth were to be fixed, one would expect a relative undersampling of regions in SssI, compared to a sample of interest that is presumably largely unmethylated. To adjust the modeled mean (in the Poisson model) for these composition effects, we estimate a normalizing factor f that accounts simultaneously for overall sequencing depth and composition. Figure S2 of Additional file 2 shows an M (log-ratio) versus A (average-log-count) plot at 50,000 randomly chosen (100bp) bins for IMR-90 compared to the fully methylated control. A clear offset from zero is visible, where the distribution of M values is skewed in the negative direction. The normalization offset f is estimated as $f = 2^{\text{median}(M_{A>q})}$, with q corresponding to a high (here, 0.998; more than 35000 points in both applications) quantile of A . In cancer samples where CNV are common, the normalization factor f is calculated from bins that originate from the most prominent copy number state

(e.g., $ccn = 4$ in LNCaP cells).

Estimation of copy number

Copy number estimates were estimated from Affymetrix SNP6.0 genotyping array data by PICNIC [51], using default parameters. PICNIC is an algorithm based on a hidden Markov model to produce absolute allelic copy number segmentation.

Details on BayMeth methodology

The methodology of BayMeth is roughly divided into two steps:

1. An empirical Bayes procedure to derive sensible prior parameters for all parameters in the model.
2. The analytical derivation of the posterior marginal distribution, posterior expectation and variance for the methylation levels. Credible intervals are derived numerically from the posterior marginal distribution.

The details for both steps are provided in Additional file 1. In practice BayMeth can be used almost as a black box within the Bioconductor package `Repitools` [48].

Details on Batman specifications

Batman is an algorithm implemented in JAVA and run from the command prompt. The original Batman can be downloaded from <http://td-blade.gurdon.cam.ac.uk/software/batman/>; we used an unreleased version “20090617” received directly from Thomas Down that had MeDIP-seq-specific enhancements; the commands used to run Batman are given at the Supplementary website.

Details on MEDIPS specifications

We used the R-Bioconductor MEDIPS version 1.4.0 and followed the available tutorial (medips.molgen.mpg.de/MEDIPS.1.0.0/MEDIPS.pdf from October 18, 2010); the detailed command sequence is given at the Supplementary website. MEDIPS returns methylation estimates in the range from zero to 1000, which we rescaled to the interval $[0, 1]$. In our comparison, we used the absolute methylation score (AMS) provided by MEDIPS.

Details on BALM specifications

BALM is an algorithm implemented in C and C++ and run from the command prompt. The original BALM can be downloaded from <http://motif.bmi.ohio-state.edu/BALM/>; We used the version 1.01. The detailed command sequence is given at the Supplementary website. BALM returns a vector of methylation estimates, one for each targeted CpG site. To obtain (100bp) bin-specific methylation profiles, we averaged the methylation estimates from all CpG sites within 100bp (upstream and downstream; total window of 200bp) from the center of our 100bp bins. For the IMR-90 data set BALM was run without an input control. To assess the effect of the missing input control, we run BALM using a sample from a normal human prostate epithelial cell line (PrEC) as input control which lead to almost identical performance results.

Software

BayMeth is fully integrated into the R-package **Repitools** and available from the Bioconductor web page <http://www.bioconductor.org/packages/release/bioc/html/Repitools.html>. Data (semi-processed), R Code for all figures and analyses are provided on http://imlspenticton.uzh.ch/robinson_lab/BayMeth/index.html.

Acronyms

DNAme DNA methylation

RRBS reduced representation bisulphite sequencing

CNV copy number variation

WGBS whole genome bisulphite sequencing

BS sodium bisulphite

MBD methyl binding domain

IMR-90 human lung fibroblast

LNCaP human prostate carcinoma

HPD highest posterior density

Authors contributions

The statistical approach was conceived and developed by AR and MDR, with biological and technical insight from ALS, CS, MM and SJC. Implementation and data analyses were done by AR with contributions from MDR. Data was collected by JZS, ALS, NM, CM and MM. AR and MDR wrote the manuscript with input from all authors. All authors read and approved the final manuscript.

Additional Files

Additional file 1 — Statistical details of BayMeth

This document describes all details of the BayMeth methodology. Two different prior distributions for the methylation level are presented, namely, a mixture of beta distributions, and a mixture of a point mass at zero, a beta distribution and a point mass at one (Dirac-beta-Dirac prior). An empirical Bayes procedure is outlined to derive prior parameters. Analytical derivation of the posterior marginal distribution and parameter estimation is described for both priors. We outline the derivations for the standard BayMeth version, i.e. taking advantage of SssI information, and for the SssI-free version.

Additional file 2 — Supplementary figures and tables

This document contains six supplementary figures and one supplementary table. Detailed descriptions are provided within the file.

Additional file 3 — BayMeth analysis of “Bock” data

This document outlines all data preparation steps performed and presents detailed R-code for the BayMeth analysis conducted using the Bioconductor package `Repitools`.

Acknowledgements

AR gratefully acknowledges funding of the “Forschungskredit” and the URPP (University Research Priority Program in Systems Biology/Functional Genomics) grant of the University of Zurich. MM acknowledges grant funding from the Swiss Cancer League (KFS-02739-02-2011). SJC gratefully acknowledges grant funding from NHMRC and NBCF. MDR acknowledges financial support from SNSF project grant (143883) and from the European Commission through the 7th Framework Collaborative Project RADIANT (Grant Agreement Number: 305626). We thank Elena Zotenko, Marcel Coolen, Giancarlo Marra, Mattia Pelizzola, Mark van de Wiel and Leonhard Held for useful discussions on the experimental, computational and statistical strategies.

References

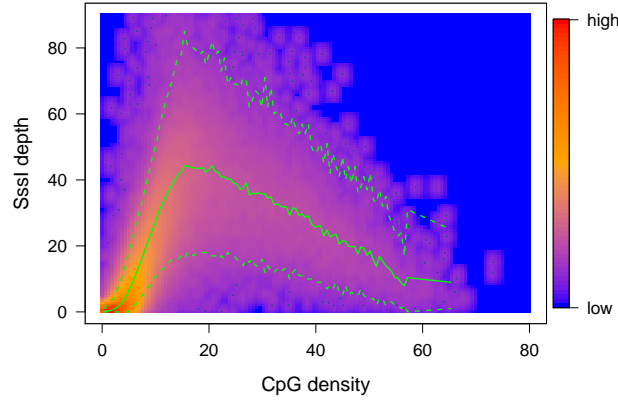
1. Jones PA, Baylin SB: **The epigenomics of cancer.** *Cell* 2007, **128**(4):683–692.
2. Slomko H, Heo HJ, Einstein FH: **Minireview: epigenetics of obesity and diabetes in humans.** *Endocrinology* 2012, **153**(3):1025–1030.
3. Clark SJ, Melki J: **DNA methylation and gene silencing in cancer: which is the guilty party?** *Oncogene* 2002, **21**(35):5380–5387.
4. Esteller M: **Cancer epigenomics: DNA methylomes and histone-modification maps.** *Nature Reviews Genetics* 2007, **8**(4):286–298.
5. Ziller MJ, Gu H, Müller F, Donaghey J, Tsai LTY, Kohlbacher O, De Jager PL, Rosen ED, Bennett DA, Bernstein BE, Gnirke A, Meissner A: **Charting a dynamic DNA methylation landscape of the human genome.** *Nature* 2013, **500**(7463):477–481.
6. Ruike Y, Imanaka Y, Sato F, Shimizu K, Tsujimoto G: **Genome-wide analysis of aberrant methylation in human breast cancer cells using methyl-DNA immunoprecipitation combined with high-throughput sequencing.** *BMC Genomics* 2010, **11**:137.
7. Stein RA: **Epigenetics—The link between infectious diseases and cancer.** *Journal of the American Medical Association* 2011, **305**(14):1484–1485.
8. Baylin SB, Jones PA: **A decade of exploring the cancer epigenome—biological and translational implications.** *Nature Reviews Cancer* 2011, **11**(10):726–734.
9. Jones PA: **Functions of DNA methylation: islands, start sites, gene bodies and beyond.** *Nature Reviews Genetics* 2012, [<http://dx.doi.org/10.1038/nrg3230>].
10. Gu H, Bock C, Mikkelsen TS, Jager N, Smith ZD, Tomazou E, Gnirke A, Lander ES, Meissner A: **Genome-scale DNA methylation mapping of clinical samples at single-nucleotide resolution.** *Nature Methods* 2010, **7**(2):133–136.
11. Laird PW: **Principles and challenges of genome-wide DNA methylation analysis.** *Nature Reviews Genetics* 2010, **11**(3):191–203.
12. Lister R, Ecker JR: **Finding the fifth base: genome-wide sequencing of cytosine methylation.** *Genome Research* 2009, **19**(6):959–966.
13. Kerick M, Fischer A, Schweiger MR: **Generation and Analysis of Genome-Wide DNA Methylation Maps.** In *Bioinformatics for High Throughput Sequencing*. Edited by Rodríguez-Ezpeleta N, Hackenberg M, Aransay AM, Springer New York 2012:151–167.
14. Clark SJ, Harrison J, Paul CL, Frommer M: **High sensitivity mapping of methylated cytosines.** *Nucleic Acids Research* 1994, **22**(15):2990–2997.
15. Bibikova M, Barnes B, Tsan C, Ho V, Klotzle B, Le JM, Delano D, Zhang L, Schroth GP, Gunderson KL, Fan JB, Shen R: **High density DNA methylation array with single CpG site resolution.** *Genomics* 2011, **98**(4):288–295.
16. Robinson MD, Statham AL, Speed TP, Clark SJ: **Protocol matters: which methylome are you actually studying?** *Epigenomics* 2010, **2**(4):587–598.
17. Hansen KD, Timp W, Bravo HC, Sabunciyar S, Langmead B, McDonald OG, Wen B, Wu H, Liu Y, Diep D, Briem E, Zhang K, Irizarry RA, Feinberg AP: **Increased methylation variation in epigenetic domains across cancer types.** *Nat. Genet.* 2011, **43**(8):768–775.
18. Lee EJ, Pei L, Srivastava G, Joshi T, Kushwaha G, Choi JH, Robertson KD, Wang X, Colbourne JK, Zhang L, Schroth GP, Xu D, Zhang K, Shi H: **Targeted bisulfite sequencing by solution hybrid selection and massively parallel sequencing.** *Nucleic Acids Research* 2011, **39**(19):e127.
19. Lee EJ, Luo J, Wilson JM, Shi H: **Analyzing the cancer methylome through targeted bisulfite sequencing.** *Cancer letters* 2012. in press.
20. Clarke J, Wu HC, Jayasinghe L, Patel A, Reid S, Bayley H: **Continuous base identification for single-molecule nanopore DNA sequencing.** *Nature Nanotechnology* 2009, **4**(4):265–270.
21. Flusberg BA, Webster DR, Lee JH, Travers KJ, Olivares EC, Clark TA, Korlach J, Turner SW: **Direct detection of DNA methylation during single-molecule, real-time sequencing.** *Nature Methods* 2010, **7**(6):461–465.

22. Down TA, Rakyan VK, Turner DJ, Flicek P, Li H, Kulesha E, Gräf S, Johnson N, Herrero J, Tomazou EM, Thorne NP, Bäckdahl L, Herberth M, Howe KL, Jackson DK, Miretti MM, Marioni JC, Birney E, Hubbard TJP, Durbin R, Tavaré S, Beck S: **A Bayesian deconvolution strategy for immunoprecipitation-based DNA methylome analysis.** *Nature Biotechnology* 2008, **26**(7):779–785.
23. Aberg KA, McClay JL, Nerella S, Xie LY, Clark SL, Hudson AD, Bukszár J, Adkins D, Consortium SS, Hultman CM, et al.: **MBD-seq as a cost-effective approach for methylome-wide association studies: demonstration in 1500 case-control samples.** *Epigenomics* 2012, **4**(6):605–621.
24. Clark C, Palta P, Joyce CJ, Scott C, Grundberg E, Deloukas P, Palotie A, Coffey AJ: **A comparison of the whole genome approach of MeDIP-seq to the targeted approach of the Infinium HumanMethylation450 BeadChip(®) for methylome profiling.** *PLoS ONE* 2012, **7**(11):e50233.
25. De Meyer T, Mampaey E, Vlemmix M, Denil S, Trooskens G, Renard JP, De Keulenaer S, Dehan P, Menschaert G, Van Criekinge W: **Quality evaluation of methyl binding domain based kits for enrichment DNA-methylation sequencing.** *PLoS ONE* 2013, **8**(3):e59068.
26. Nair SS, Coolen MW, Stirzaker C, Song JZ, Statham AL, Strbenac D, Robinson MD, Clark SJ: **Comparison of methyl-DNA immunoprecipitation (MeDIP) and methyl-CpG binding domain (MBD) protein capture for genome-wide DNA methylation analysis reveal CpG sequence coverage bias.** *Epigenetics* 2011, **6**:34–44.
27. Serre D, Lee BH, Ting AH: **MBD-isolated genome sequencing provides a high-throughput and comprehensive survey of DNA methylation in the human genome.** *Nucleic Acids Research* 2010, **38**(2):391–399.
28. Chavez L, Jozefczuk J, Grimm C, Dietrich J, Timmermann B, Lehrach H, Herwig R, Adjaye J: **Computational analysis of genome-wide DNA methylation during the differentiation of human embryonic stem cells along the endodermal lineage.** *Genome Research* 2010, **20**(10):1441–1450.
29. Lan X, Adams C, Landers M, Dudas M, Krissinger D, Marnellos G, Bonneville R, Xu M, Wang J, Huang THM, Meredith G, Jin VX: **High resolution detection and analysis of CpG dinucleotides methylation using MBD-seq technology.** *PLoS ONE* 2011, **6**(7):e22226.
30. Feber A, Wilson GA, Zhang L, Presneau N, Idowu B, Down TA, Rakyan VK, Noon LA, Lloyd AC, Stupka E, Schiza V, Teschendorff AE, Schroth GP, Flanagan A, Beck S: **Comparative methylome analysis of benign and malignant peripheral nerve sheath tumors.** *Genome Research* 2011, **21**(4):515–524.
31. Stevens M, Cheng JB, Li D, Xie M, Hong C, Maire CL, Ligon KL, Hirst M, Marra MA, Costello JF, Wang T: **Estimating absolute methylation levels at single-CpG resolution from methylation enrichment and restriction enzyme sequencing methods.** *Genome Research* 2013, **23**(9):1541–1553.
32. Bock C, Tomazou EM, Brinkman A, Müller F, Simmer F, Gu H, Jäger N, Gnirke A, Stunnenberg HG, Meissner A: **Genome-wide mapping of DNA methylation: a quantitative technology comparison.** *Nature Biotechnology* 2010, **28**:1106–1114.
33. Robinson MD, Strbenac D, Stirzaker C, Statham AL, Song JZ, Speed TP, Clark SJ: **Copy-number-aware differential analysis of quantitative DNA sequencing data.** *Genome Research* 2012, [<http://dx.doi.org/10.1101/gr.139055.112>].
34. Fader PS, Hardie BGS: **A note on modelling underreported Poisson counts.** *Journal of Applied Statistics* 2000, **27**(8):953–964.
35. Abramowitz M, Stegun IA: *Handbook of Mathematical functions with Formulas, Graphs and Mathematical Tables.* New York: Dover Publications 1972.
36. Pelizzola M, Koga Y, Urban AE, Krauthammer M, Weissman S, Halaban R, Molinaro AM: **MEDME: an experimental and analytical methodology for the estimation of DNA methylation levels based on microarray derived MeDIP-enrichment.** *Genome Research* 2008, **18**(10):1652–1659.
37. Robinson MD, Stirzaker C, Statham AL, Coolen MW, Song JZ, Nair SS, Strbenac D, Speed TP, Clark SJ: **Evaluation of affinity-based genome-wide DNA methylation data: effects of CpG density, amplification bias, and copy number variation.** *Genome Research* 2010, **20**(12):1719–1729.
38. Schmittlein DC, Bemmaor AC, Morrison DG: **Why does the NBD model work? Robustness in representing product purchases, brand purchases and imperfectly recorded purchases.** *Marketing Science* 1985, **4**:255–266.

39. Winkelmann R: **Markov chain Monte Carlo analysis of underreported count data with an application to worker absenteeism.** *Empirical Economics* 1996, **21**(4):575–587.
40. Lister R, Pelizzola M, Dowen RH, Hawkins RD, Hon G, Tonti-Filippini J, Nery JR, Lee L, Ye Z, Ngo QM, Edsall L, Antosiewicz-Bourget J, Stewart R, Ruotti V, Millar AH, Thomson JA, Ren B, Ecker JR: **Human DNA methylomes at base resolution show widespread epigenomic differences.** *Nature* 2009, **462**(7271):315–322.
41. Houseman EA, Christensen BC, Karagas MR, Wrensch MR, Nelson HH, Wiemels JL, Zheng S, Wiencke JK, Kelsey KT, Marsit CJ: **Copy number variation has little impact on bead-array-based measures of DNA methylation.** *Bioinformatics* 2009, **25**(16):1999–2005.
42. Pickrell J, Gaffney D, Gilad Y, Pritchard J: **False positive peaks in ChIP-seq and other sequencing-based functional assays caused by unannotated high copy number regions.** *Bioinformatics* 2011, **27**(15):2144–2146.
43. Taiwo O, Wilson GA, Morris T, Seisenberger S, Reik W, Pearce D, Beck S, Butcher LM: **Methylome analysis using MeDIP-seq with low DNA concentrations.** *Nature Protocols* 2012, **7**(4):617–636.
44. Carvalho RH, Haberle V, Hou J, van Gent T, Thongjuea S, van Ijcken W, Kockx C, Brouwer R, Rijkers E, Sieuwerts A, Foekens J, van Vroonhoven M, Aerts J, Grosveld F, Lenhard B, Philipsen S: **Genome-wide DNA methylation profiling of non-small cell lung carcinomas.** *Epigenetics Chromatin* 2012, **5**:9.
45. Hansen KD, Irizarry RA, Wu Z: **Removing technical variability in RNA-seq data using conditional quantile normalization.** *Biostatistics* 2012, **13**(2):204–216.
46. Wu G, Yi N, Absher D, Zhi D: **Statistical quantification of methylation levels by next-generation sequencing.** *PLoS ONE* 2011, **6**(6):e21034.
47. Rue H, Held L: *Gaussian Markov Random Fields: Theory and Applications.* London: Chapman & Hall/CRC Press 2005.
48. Statham AL, Strbenac D, Coolen MW, Stirzaker C, Clark SJ, Robinson MD: **Repitools: an R package for the analysis of enrichment-based epigenomic data.** *Bioinformatics* 2010, **26**(13):1662–1663.
49. Hansen KD, Aryee M: *minfi: Analyze Illumina's 450k methylation arrays.* [R package version 1.3.3].
50. Robinson MD, Oshlack A: **A scaling normalization method for differential expression analysis of RNA-seq data.** *Genome Biology* 2010, **11**(3):R25.
51. Greenman CD, Bignell G, Butler A, Edkins S, Hinton J, Beare D, Swamy S, Santarius T, Chen L, Widaa S, Futreal PA, Stratton MR: **PICNIC: an algorithm to predict absolute allelic copy number variation with microarray cancer data.** *Biostatistics* 2010, **11**:164–175.

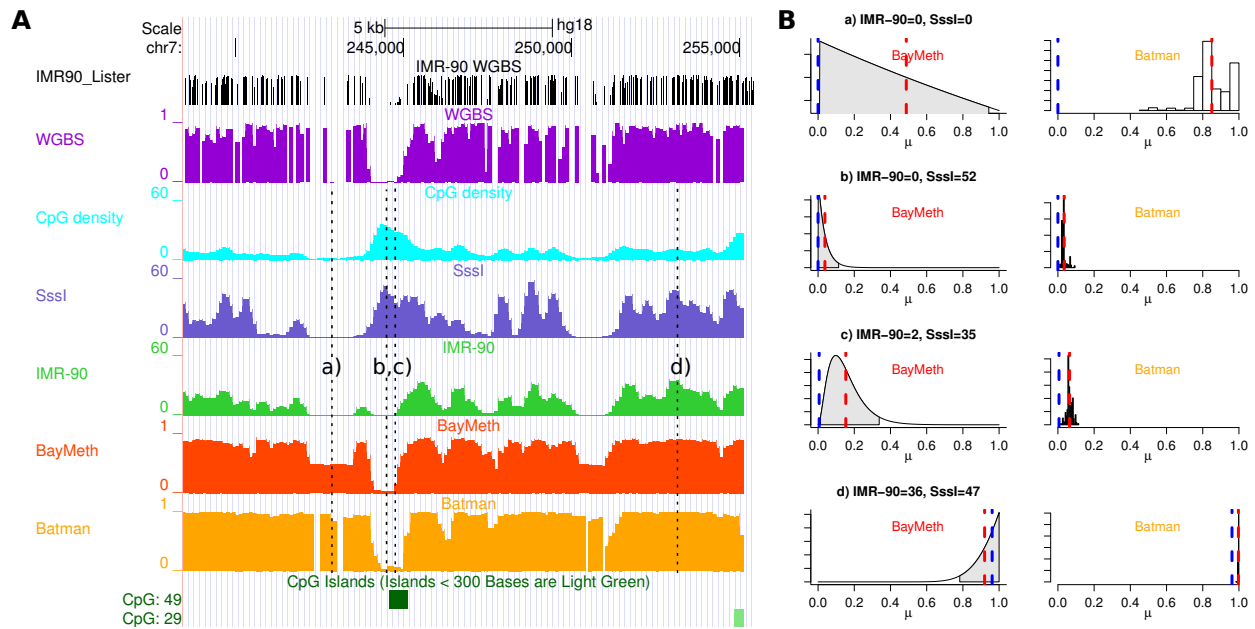
Figures

Figure 1 - Sssl read depth versus CpG-density together with prior predictive distribution



Smoothed color density representation of Sssl read depth versus CpG-density together with mean (green solid line), 2.5% and 97.5%-quantile (green dashed lines) of the prior predictive distribution for the Sssl control sample. The parameters of this negative binomial distribution are derived using an empirical Bayes approach by maximizing the joint marginal distribution of the IMR-90 and Sssl control counts stratified into 100 CpG-density groups. Only counts from bins with a mappability larger than 0.75 were considered.

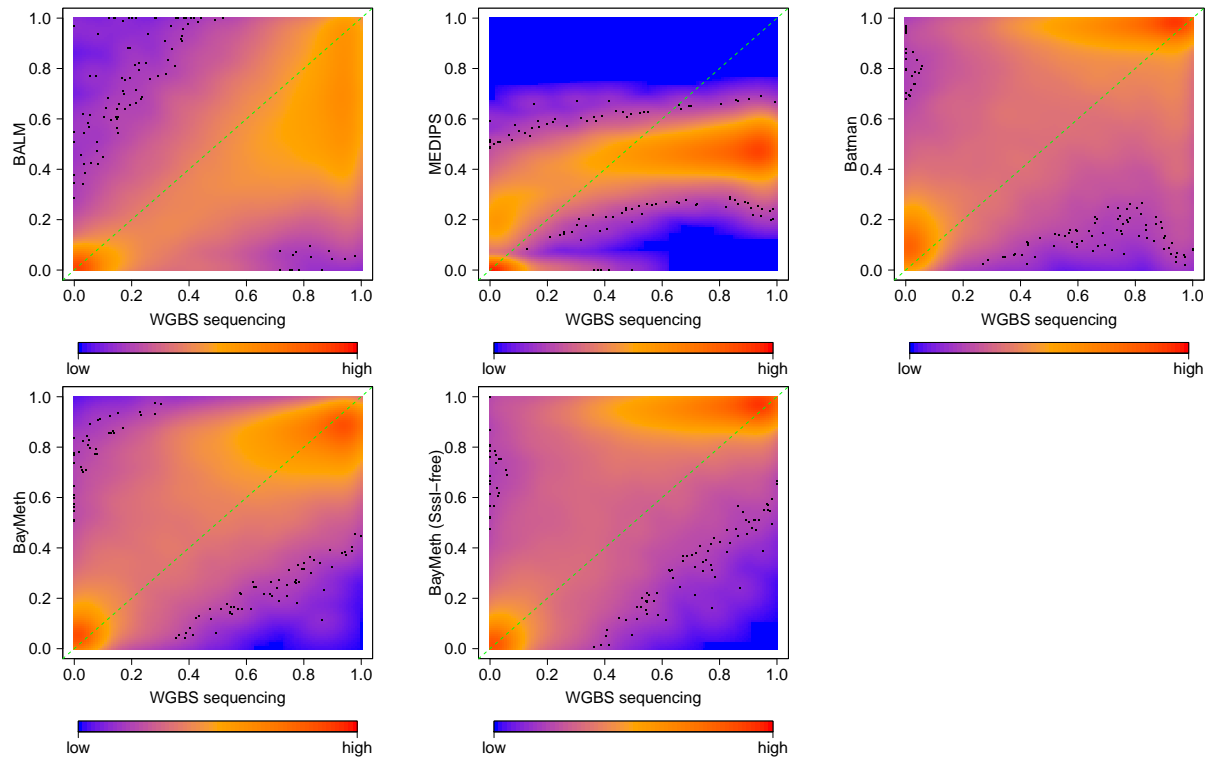
Figure 2 - Example data tracks for IMR-90 chromosome 7



Panel A: Shown are the WGBS methylome (black) per CpG-site and per 100bp bin (purple) as obtained by Lister and others [40]. CpG-density (light blue), and read counts for Sssl-treated DNA (blue) and IMR-90

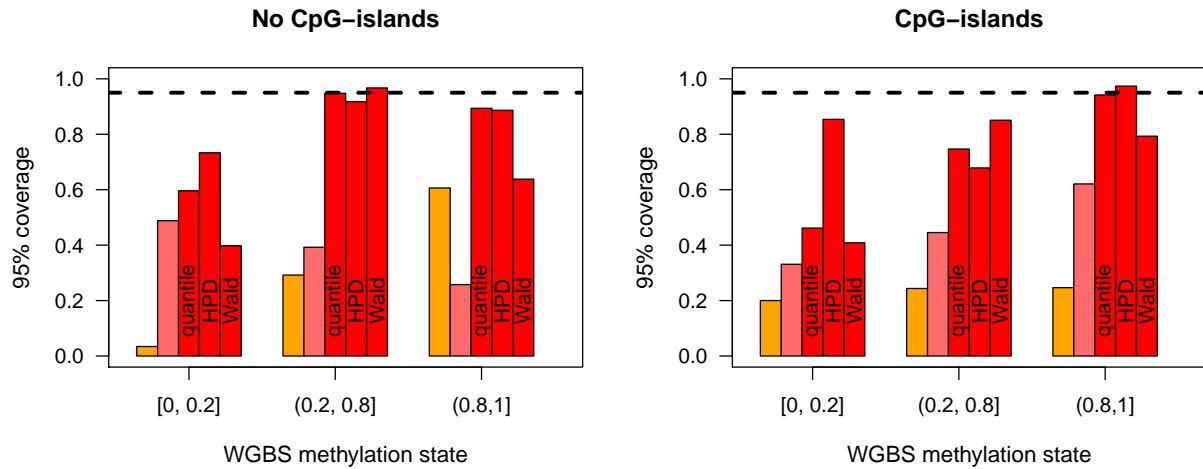
cells (green) obtained by MBD-seq based on 100bp non-overlapping bins are shown. Methylation estimates for BayMeth (red) and Batman (orange) are provided. Panel B: For 4 specific bins of panel A (denoted a, b, c, d) detailed posterior information of BayMeth and Batman is provided. For BayMeth posterior marginals together with 95% highest-posterior-density (HPD) credible intervals (grey-shaded) are shown. The posterior samples obtained by Batman are plotted as histograms. For both approaches the posterior mean is indicated (red dashed line) together with the “true” WGBS derived methylation estimate (blue dashed line).

Figure 3 - Regional methylation estimates for IMR-90 chromosome 7



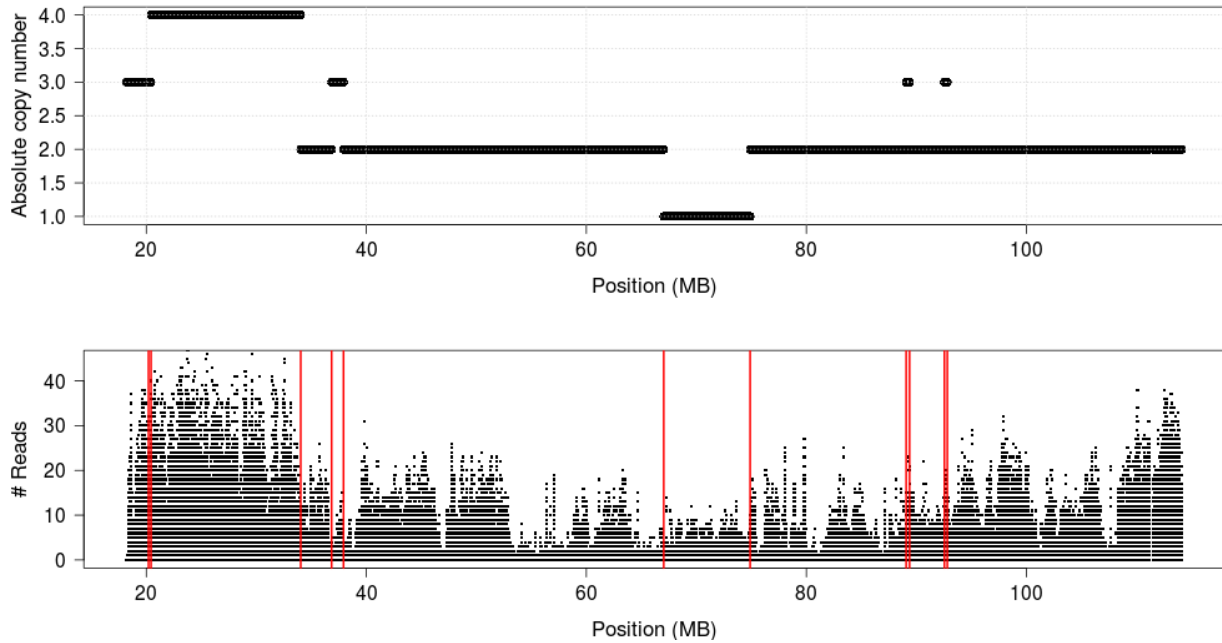
Smoothed color density representation of regional DNAm estimates of BALM, MEDIPS, Batman, BayMeth and BayMeth ignoring SssI information, respectively, plotted against WGBS methylation levels for the 75% of bins with the largest depth in the truth (cutoff are 33 reads) where the depth in the SssI control is (27, 168]. In addition the $y = x$ line (green dashed line) is shown. Black points indicate outliers.

Figure 4 - Coverage probabilities stratified by CpG island status and true methylation level



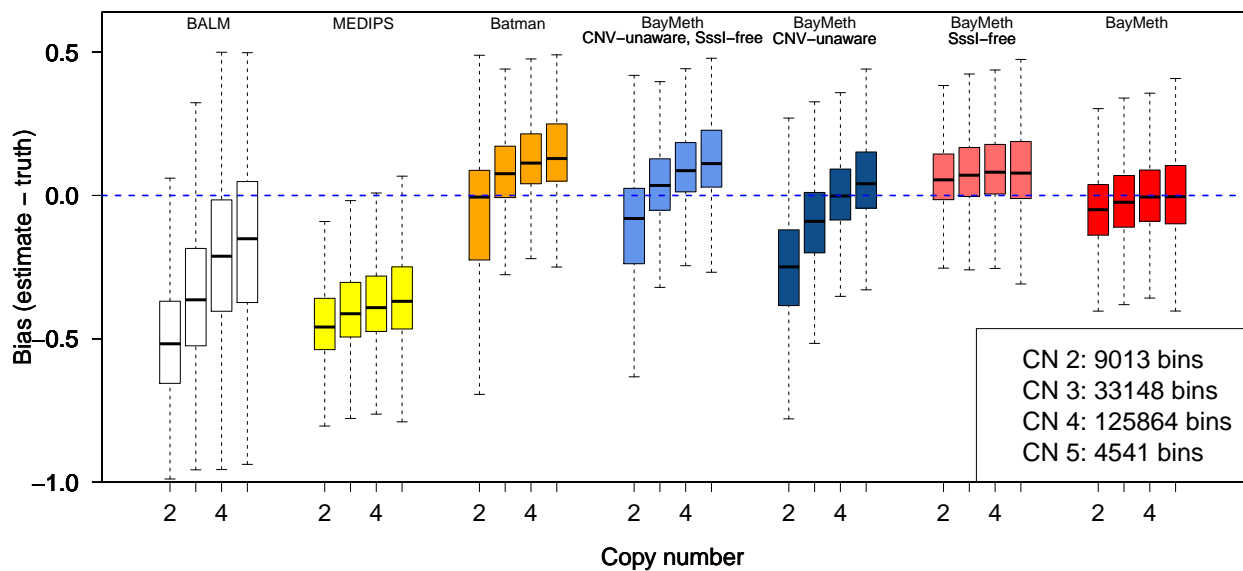
Coverage probabilities (frequency in which the true value is within a predefined credible interval) at 95% level are shown for the 75% of bins with the largest depth in the truth (cutoff are 33 reads) for Batman (orange), BayMeth ignoring SssI control information (light red), and BayMeth (red). Three different types (quantile-based, Wald, HPD) of credible intervals are shown for BayMeth, while for Batman and the SssI-free version of BayMeth only quantile-based intervals are available. MEDIPS and Balm do not return any uncertainty estimates. The nominal coverage value is indicated (black dashed line) as a reference. Genomic regions are stratified by CpG-density using the threshold of 12.46 which separates CpG islands from non-CpG islands, compare Figure S1 of Additional file 2. Further stratification by the true methylation level as derived from WGBS [40] is provided.

Figure 5 - Relation between copy number state and regional affinity enrichment



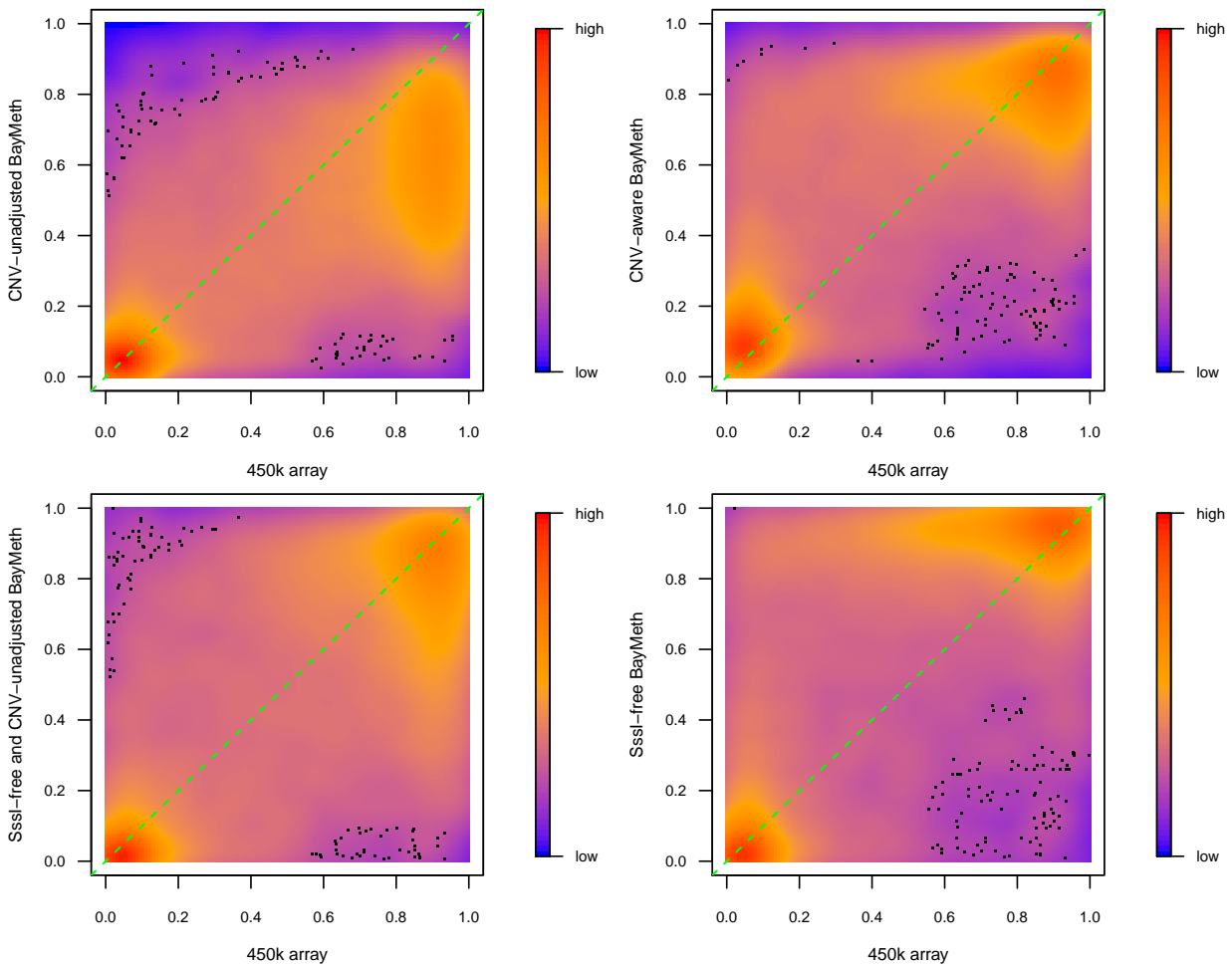
Top: Copy number estimates of LNCaP cell line obtained by the PICNIC [51] algorithm for 100bp bins across human chromosome 13 with a mappability of at least 75%. Bottom: Read counts of affinity capture sequencing data for the same bins.

Figure 6 - Bias of LNCaP methylation estimates compared to 450k array beta values



Boxplot of bias (Estimated methylation level - 450K array beta value) for BALM (white), MEDIPS (yellow), Batman (orange), CNV-unaware and SssI-free BayMeth (light blue), CNV-unaware BayMeth (dark blue), SssI-free but CNV-aware BayMeth (light red) and CNV-aware BayMeth (red) stratified by the most prominent copy number. (Outliers are not shown.) Taking SssI information into account a uniform prior for the methylation level was used, in the SssI-free version a Dirac-Beta-Dirac mixture with weights fixed to 0.1, 0.8, 0.1 was used. The results are shown genome-wide for 100bp bins with at least 75% mappability and where the true methylation estimate is larger than 0.5. A threshold of 13 is applied for the depth of SssI. The blue dashed line indicates a bias of zero.

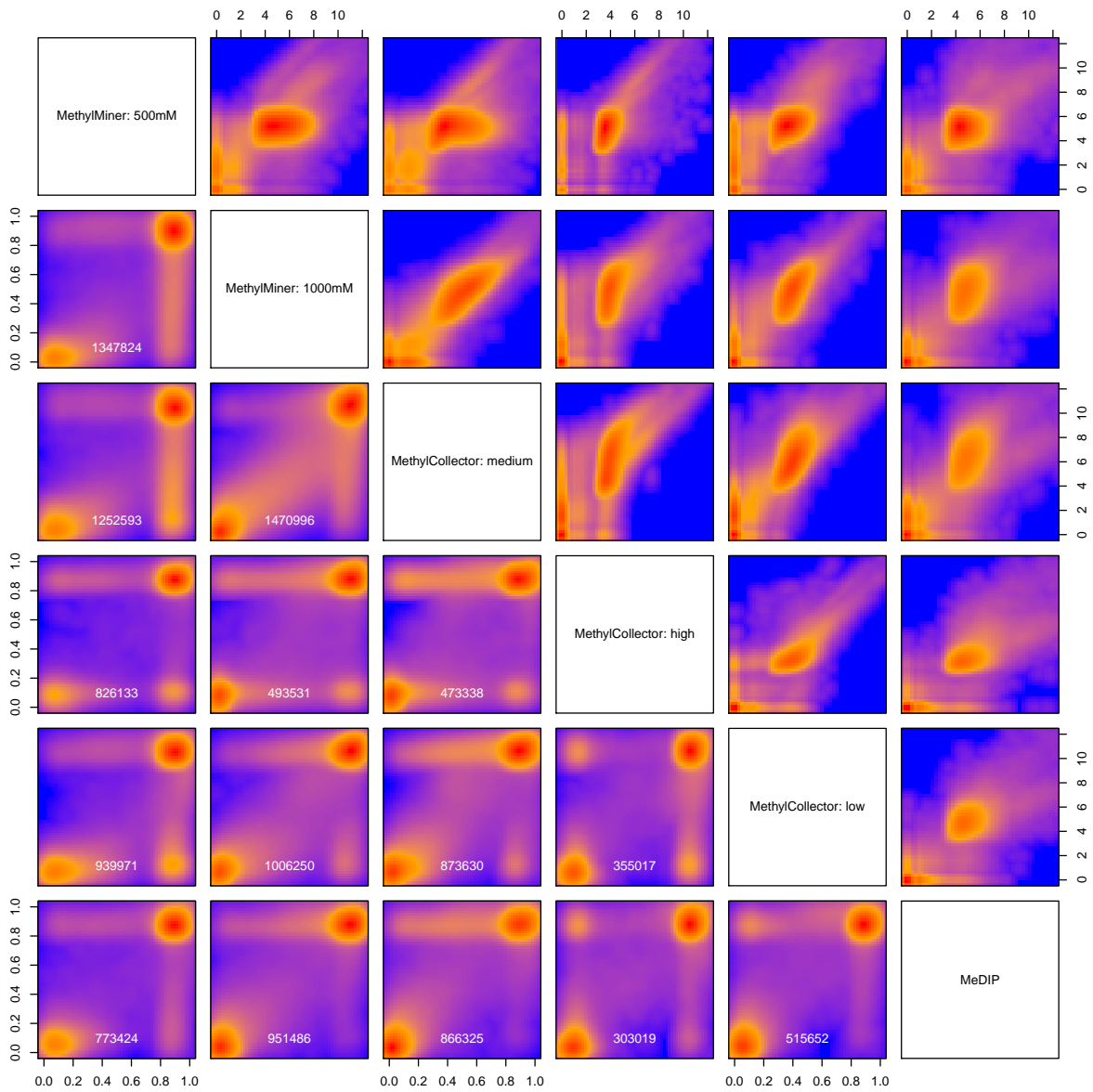
Figure 7 - Effect of adjusting for CNV in LNCaP cell line



Smoothed color density representation of methylation estimates for copy number state two derived by BayMeth compared to 450k array beta values. A threshold of 13 is applied for the depth of SssI, which

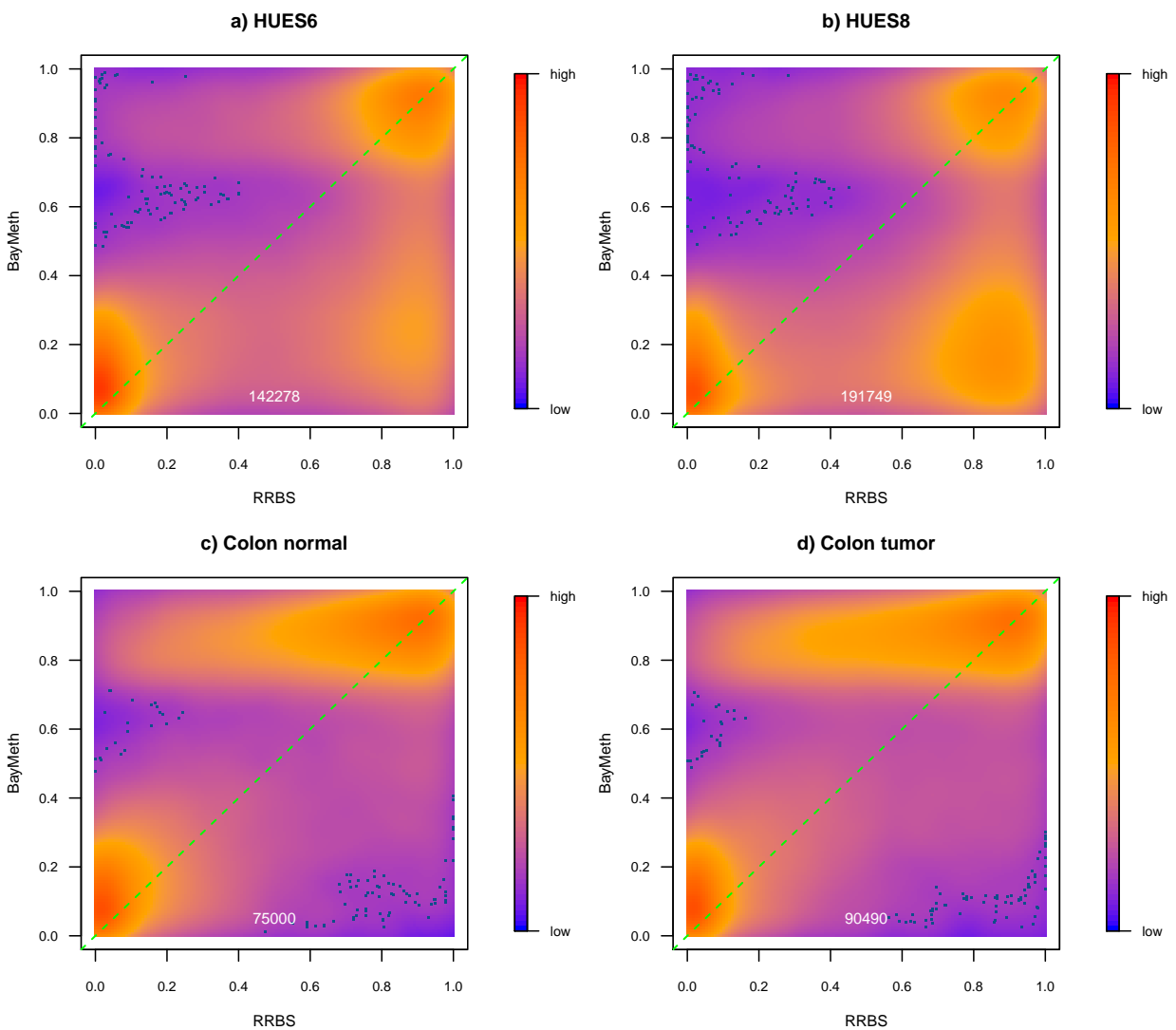
leads to 61969 bins, of which we have for 18010 100bp-bins a beta values and BayMeth estimate. In addition the $y = x$ line (green dashed line) is shown. Black points indicate outliers. Top-Left: CNV-unaware BayMeth; Top-Right: CNV-aware BayMeth; Bottom-Left: SssI-free and CNV-unaware BayMeth; Bottom-Right: SssI-free BayMeth.

Figure 8 - Comparison of raw IMR-90 data and methylation estimates obtained by different methylation kits



Genomic bins (100bp), with a mappability larger than 75%, are selected for which the predicted HPD credible interval width is smaller than 0.4. For these bins the upper triangular panels show a smoothed color density representation (going from blue representing low density to red for high density) of the raw counts and the lower triangular panels the estimated methylation levels obtained by different methylation kits against each other. The number of bins included is given in the panels of the lower triangular in white.

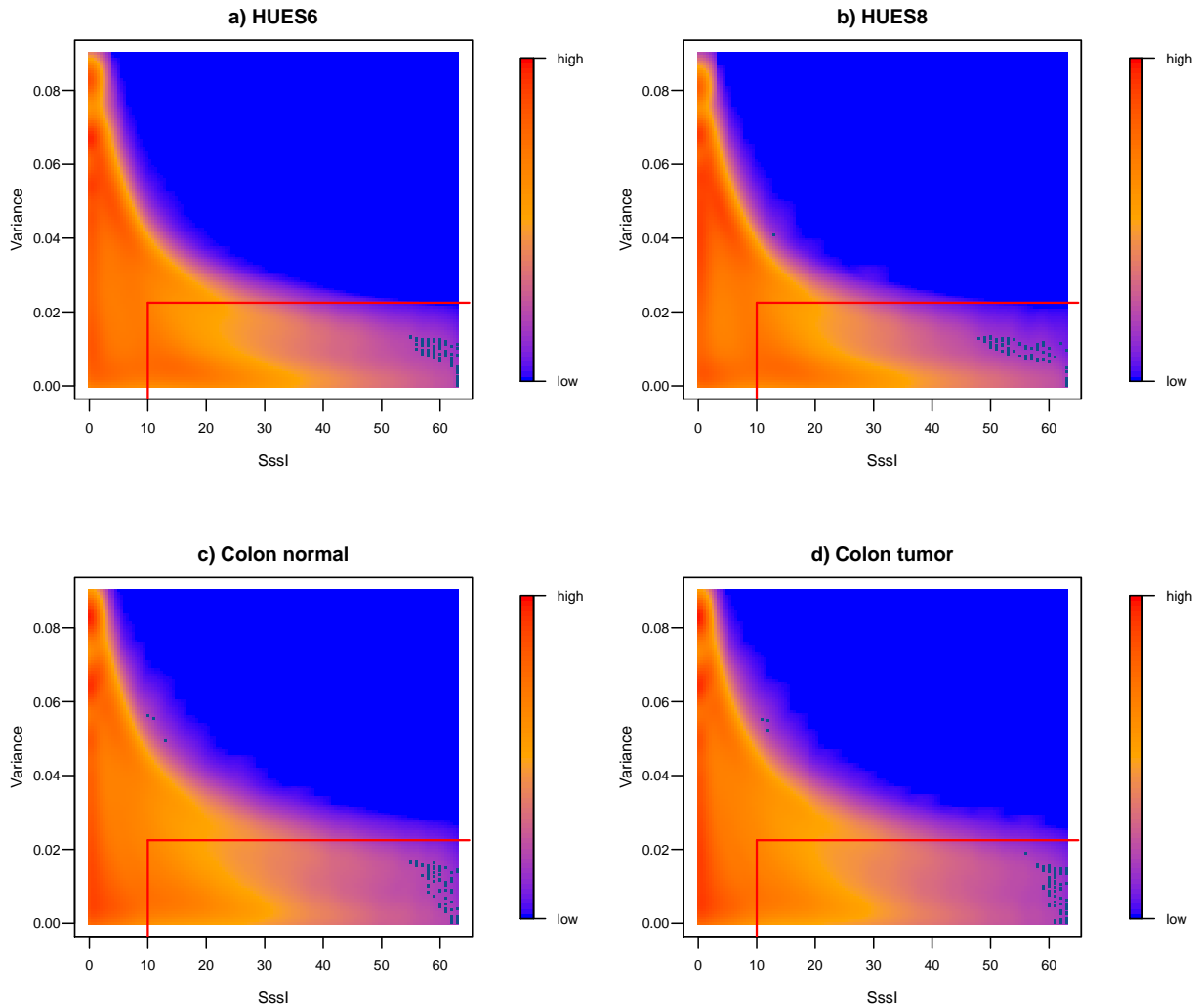
Figure 9 - Regional methylation estimates for samples of Bock data



Smoothed color density representation of regional DNAm estimates of BayMeth, plotted against RRBS methylation levels, where the estimated standard deviation of BayMeth is smaller than 0.15 for bins with more than 20 reads for RRBS and at least a depth of 10 in the SssI control. The number of bins included

in the plot is shown at the bottom center of the panels.

Figure 10 - Regional variance estimates versus Sssl control for Bock data



Smooth color density representation of variance estimates obtained by BayMeth versus number of reads in the Sssl control for a read depth larger than 20 in RRBS. The red box contains the bins used in Figure 9 having at least a depth of 10 in Sssl and a standard deviation smaller than 0.15, i.e. a variance smaller than 0.025.

Tables

Table 1 - Performance assessment for IMR-90 analysis (chromosome 7)

Results are shown for bins with a truth depth larger than the 25% quantile (cutoff are 33 reads), stratified into five groups by SssI depth. Shown are the number of bins per group, mean bias, MSE, Spearman correlation and coverage probabilities at 95% level.

SssI depth	#Bins	Method	Bias	MSE	Cor	Wald	HPD	quantile
[0, 4]	305638	BayMeth	-0.04	0.08	0.36	0.74	0.89	0.89
		BayMeth (SssI-free)	-0.19	0.20	0.23	—	—	0.24
		Batman	0.22	0.14	0.31	—	—	0.43
		MEDIPS	-0.38	0.26	0.29	—	—	—
		BALM	-0.48	0.33	0.32	—	—	—
(4, 7]	22196	BayMeth	0.05	0.05	0.65	0.84	0.88	0.87
		BayMeth (SssI-free)	-0.01	0.08	0.42	—	—	0.68
		Batman	0.16	0.07	0.61	—	—	0.34
		MEDIPS	-0.23	0.11	0.45	—	—	—
		BALM	-0.27	0.15	0.60	—	—	—
(7, 14]	28871	BayMeth	0.06	0.04	0.69	0.84	0.86	0.86
		BayMeth (SssI-free)	0.02	0.05	0.57	—	—	0.79
		Batman	0.16	0.07	0.65	—	—	0.28
		MEDIPS	-0.21	0.10	0.49	—	—	—
		BALM	-0.21	0.11	0.66	—	—	—
(14, 27]	28928	BayMeth	0.05	0.03	0.76	0.81	0.85	0.82
		BayMeth (SssI-free)	0.08	0.04	0.72	—	—	0.70
		Batman	0.15	0.06	0.73	—	—	0.23
		MEDIPS	-0.20	0.09	0.59	—	—	—
		BALM	-0.15	0.07	0.75	—	—	—
(27, 168]	28719	BayMeth	0.02	0.03	0.79	0.73	0.86	0.78
		BayMeth (SssI-free)	0.11	0.04	0.77	—	—	0.48
		Batman	0.11	0.05	0.75	—	—	0.20
		MEDIPS	-0.22	0.10	0.67	—	—	—
		BALM	-0.14	0.06	0.76	—	—	—

Table 2 - Copy number specific offset

Copy number specific offsets defined as $f \times \frac{cn_i}{ccn}$ derived for 100bp non-overlapping bins of LNCaP autosomes, which have a mappability of at least 75%. Note, that f is only derived based on bins with the most common copy number state four.

	1	2	3	4	5	6	7	8
Combined offset	0.178	0.356	0.534	0.712	0.889	1.067	1.245	1.423

Table 3 - Performance assessment for LNCaP analysis by copy number

Results are shown for 100bp-bins with a mappability of at least 0.75 stratified into the four most frequent copy number states. A threshold of 13 is applied for the depth of the SssI-control. Four BayMeth four

different variations are shown, depending on whether SssI-control information is used and whether copy number information is integrated. Taking SssI information into account a uniform prior for the methylation level was used, in the SssI-free version a Dirac-Beta-Dirac mixture with weights fixed to 0.1, 0.8, 0.1 was used. Shown are the number of bins per copy number state, mean bias, MSE and Spearman correlation.

Copy number	#Bins	Method	Bias	MSE	Cor
2	18010	BayMeth	0.04	0.04	0.78
		BayMeth (SssI-free)	0.08	0.05	0.79
		BayMeth (CNV-unaware)	-0.11	0.06	0.78
		BayMeth (SssI-free, CNV-unaware)	-0.05	0.05	0.79
		Batman	0.03	0.06	0.74
		MEDIPS	-0.23	0.11	0.76
		BALM	-0.29	0.16	0.78
3	65982	BayMeth	0.05	0.04	0.80
		BayMeth (SssI-free)	0.09	0.05	0.80
		BayMeth (CNV-unaware)	-0.01	0.04	0.80
		BayMeth (SssI-free, CNV-unaware)	0.05	0.04	0.80
		Batman	0.11	0.06	0.77
		MEDIPS	-0.19	0.09	0.76
		BALM	-0.20	0.10	0.79
4	256074	BayMeth	0.05	0.04	0.81
		BayMeth (SssI-free)	0.09	0.05	0.81
		BayMeth (CNV-unaware)	0.05	0.04	0.81
		BayMeth (SssI-free, CNV-unaware)	0.11	0.06	0.81
		Batman	0.16	0.08	0.79
		MEDIPS	-0.17	0.09	0.76
		BALM	-0.12	0.07	0.80
5	11790	BayMeth	0.04	0.03	0.83
		BayMeth (SssI-free)	0.07	0.05	0.82
		BayMeth (CNV-unaware)	0.09	0.04	0.83
		BayMeth (SssI-free, CNV-unaware)	0.12	0.06	0.82
		Batman	0.18	0.08	0.80
		MEDIPS	-0.12	0.07	0.80
		BALM	-0.08	0.05	0.82

Additional file 1 — Statistical details of BayMeth

The methodology of BayMeth is roughly divided into two steps: 1) An empirical Bayes procedure to derive parameters for the prior distributions of all parameters in the model. 2) The analytical derivation of the posterior marginal distribution, posterior expectation and variance for the methylation levels. Credible intervals are derived numerically from the posterior marginal distribution. Recall the model formulation provided in the main text:

$$y_{iS} | \mu_i, \lambda_i \sim \text{Poisson} \left(f \times \frac{\text{cn}_i}{\text{ccn}} \times \mu_i \times \lambda_i \right), \text{ and}$$
$$y_{iC} | \lambda_i \sim \text{Poisson}(\lambda_i),$$

Prior specification

For λ_i we assume a gamma prior distribution with parameters α and β :

$$\lambda_i | \alpha, \beta = \frac{\beta^\alpha}{\Gamma(\alpha)} \lambda_i^{\alpha-1} \exp(-\beta \lambda_i), \lambda_i > 0, \alpha, \beta > 0.$$

The methylation level μ_i has support from zero to one. We consider two groups of prior distributions:

- a mixture of beta distributions, i.e., $\mu_i \sim \sum_{m=1}^M w_m \text{Be}(a_m, b_m)$, where in its simplest form $M = 1$. (The default configuration of BayMeth is $M = 1$ and $(a = a_m = b = b_m = 1)$, i.e., a uniform distribution from zero to one.)
- a mixture of a point mass at zero, a beta distribution and a point mass at one. We call this the Dirac-Beta-Dirac (DBD) prior distribution, which has the density

$$p(\mu_i) = w_0 \delta_0 + w_1 \text{Be}(\mu_i; a, b) + w_2 \delta_1, \quad (4)$$

where

$$\delta_0 = \begin{cases} 0 & \text{if } \mu_i \neq 0 \\ 1 & \text{if } \mu_i = 0 \end{cases}, \quad \delta_1 = \begin{cases} 0 & \text{if } \mu_i \neq 1 \\ 1 & \text{if } \mu_i = 1 \end{cases}$$

and $w_0 + w_1 + w_2 = 1$.

Marginal distribution

The empirical Bayes approach is based on the maximization of the marginal distribution. For ease of readability let $E = f \times \frac{cn_i}{ccn}$. The joint marginal distribution of y_{iS}, y_{iC} results as:

$$\begin{aligned}
p(y_{iS}, y_{iC}) &= \int \int p(y_{iS}|\mu_i, \lambda_i)p(y_{iC}|\lambda_i)p(\lambda_i)p(\mu_i)d\lambda_i d\mu_i \\
&= \int_0^1 p(\mu_i) \left[\int_0^\infty p(y_{iS}|\mu_i, \lambda_i)p(y_{iC}|\lambda_i)p(\lambda_i)d\lambda_i \right] d\mu_i \\
&= \int_0^1 p(\mu_i) \left[\int_0^\infty \frac{(E\mu_i\lambda_i)^{y_{iS}} \lambda_i^{y_{iC}}}{y_{iS}!y_{iC}!} \exp(-E\mu_i\lambda_i) \times \exp(-\lambda_i) \times \frac{\beta^\alpha}{\Gamma(\alpha)} \lambda_i^{\alpha-1} \exp(-\beta\lambda_i)d\lambda_i \right] d\mu_i \\
&= \int_0^1 p(\mu_i) \left[\frac{(E\mu_i)^{y_{iS}}}{y_{iS}!y_{iC}!} \frac{\beta^\alpha}{\Gamma(\alpha)} \int_0^\infty \lambda_i^{y_{iS}+y_{iC}+\alpha-1} \exp(-(E\mu_i+1+\beta)\lambda_i) d\lambda_i \right] d\mu_i \\
&= \int_0^1 p(\mu_i) \left[\frac{(E\mu_i)^{y_{iS}}}{y_{iS}!y_{iC}!} \frac{\beta^\alpha}{\Gamma(\alpha)} \frac{\Gamma(y_{iS}+y_{iC}+\alpha)}{(E\mu_i+1+\beta)^{y_{iS}+y_{iC}+\alpha}} \right] d\mu_i \\
&= \frac{E^{y_{iS}}}{y_{iS}!y_{iC}!} \frac{\beta^\alpha}{\Gamma(\alpha)} \Gamma(y_{iS}+y_{iC}+\alpha) \int_0^1 p(\mu_i) \frac{\mu_i^{y_{iS}}}{(E\mu_i+1+\beta)^{y_{iS}+y_{iC}+\alpha}} d\mu_i
\end{aligned}$$

What is left, is to choose a prior for μ_i , that means to specify $p(\mu_i)$.

(Mixture of) beta distribution for the methylation level

Consider the simple case where the number of mixture components is one, so that $\mu_i \sim \text{Be}(a, b)$,

i.e. $p(\mu_i) = \frac{\Gamma(a+b)}{\Gamma(a)\Gamma(b)} \mu_i^{a-1} (1-\mu_i)^{b-1}$, $a, b > 0$. (For a uniform distribution $a = b = 1$). Then

$$\begin{aligned}
p(y_{iS}, y_{iC}) &= \frac{\Gamma(y_{iS}+y_{iC}+\alpha)}{\Gamma(\alpha)y_{iS}!y_{iC}!} \frac{\Gamma(a+b)}{\Gamma(a)\Gamma(b)} E^{y_{iS}} \beta^\alpha \int_0^1 \frac{\mu_i^{y_{iS}+a-1} (1-\mu_i)^{b-1}}{(E\mu_i+1+\beta)^{y_{iS}+y_{iC}+\alpha}} d\mu_i \\
&= \frac{\Gamma(y_{iS}+y_{iC}+\alpha)}{\Gamma(\alpha)y_{iS}!y_{iC}!} \frac{\Gamma(a+b)}{\Gamma(a)\Gamma(b)} E^{y_{iS}} \frac{\beta^\alpha}{(E+1+\beta)^{y_{iS}+y_{iC}+\alpha}} \int_0^1 \frac{\mu_i^{y_{iS}+a-1} (1-\mu_i)^{b-1}}{\frac{(E\mu_i+1+\beta)^{y_{iS}+y_{iC}+\alpha}}{(E+1+\beta)^{y_{iS}+y_{iC}+\alpha}}} d\mu_i \\
&= \frac{\Gamma(y_{iS}+y_{iC}+\alpha)}{\Gamma(\alpha)y_{iS}!y_{iC}!} \frac{\Gamma(a+b)}{\Gamma(a)\Gamma(b)} E^{y_{iS}} \frac{\beta^\alpha}{(\beta+1+E)^{y_{iS}+y_{iC}+\alpha}} \int_0^1 \frac{\mu_i^{y_{iS}+a-1} (1-\mu_i)^{b-1}}{\left(1 - \frac{E}{E+1+\beta} \cdot (1-\mu_i)\right)^{y_{iS}+y_{iC}+\alpha}} d\mu_i \tag{5} \\
&\stackrel{*}{=} \frac{\Gamma(y_{iS}+y_{iC}+\alpha)}{\Gamma(\alpha)y_{iS}!y_{iC}!} \frac{\Gamma(a+b)}{\Gamma(a)\Gamma(b)} E^{y_{iS}} \frac{\beta^\alpha}{(\beta+1+E)^{y_{iS}+y_{iC}+\alpha}} \int_0^1 \frac{(1-t_i)^{y_{iS}+a-1} t_i^{b-1}}{\left(1 - \frac{E}{E+1+\beta} \cdot t_i\right)^{y_{iS}+y_{iC}+\alpha}} dt_i \\
&= \frac{\Gamma(y_{iS}+y_{iC}+\alpha)}{\Gamma(\alpha)y_{iS}!y_{iC}!} \left(\frac{\beta}{\beta+1+E}\right)^\alpha \left(\frac{E}{\beta+1+E}\right)^{y_{iS}} \left(\frac{1}{\beta+1+E}\right)^{y_{iC}} \frac{\Gamma(a+b)\Gamma(y_{iS}+a)}{\Gamma(a)\Gamma(y_{iS}+a+b)} \times \\
&\quad {}_2F_1\left(y_{iS}+y_{iC}+\alpha, b; y_{iS}+a+b; \frac{E}{\beta+1+E}\right).
\end{aligned}$$

In the step marked with * we substituted $(1-\mu_i)$ with t_i , where $dt_i = -d\mu_i$, to get the desired form of the Gauss hypergeometric function (the limits of the integral stay thereby unchanged), which is defined by:

$${}_2F_1(a, b; c; z) = \frac{\Gamma(c)}{\Gamma(b)\Gamma(c-b)} \int_0^1 t^{b-1} (1-t)^{c-b-1} (1-zt)^{-a} dt, \quad c > b > 0$$

where $|z| < 1$ is the radius of convergence [35, see page 558]. (Note, $|z| = |E/(\beta + 1 + E)| < 1$ in (5), so that convergence is granted). Model (5) is similar to the beta binomial (BB)/negative binomial (NB) model derived in [38] and [34].

Using a mixture of M beta distributions as prior distribution for μ_i , i.e. $\mu_i \sim \sum_{m=1}^M w_m \text{Be}(a_m, b_m)$, where $0 \leq w_m \leq 1$, for all $m = 1, \dots, M$, and $\sum_{m=1}^M w_m = 1$ we get:

$$p(y_{iS}, y_{iC}) = \frac{\Gamma(y_{iS} + y_{iC} + \alpha)}{\Gamma(\alpha)y_{iS}!y_{iC}!} \left(\frac{\beta}{\beta + 1 + E}\right)^\alpha \left(\frac{E}{\beta + 1 + E}\right)^{y_{iS}} \left(\frac{1}{\beta + 1 + E}\right)^{y_{iC}} \times W \quad (6)$$

with

$$W = \sum_{m=1}^M \left[w_m \cdot \frac{\Gamma(a_m + b_m)\Gamma(y_{iS} + a_m)}{\Gamma(a_m)\Gamma(y_{iS} + a_m + b_m)} \times {}_2F_1 \left(y_{iS} + y_{iC} + \alpha, b_m; y_{iS} + a_m + b_m; \frac{E}{\beta + 1 + E} \right) \right].$$

Of note, ignoring the SssI information the marginal distribution changes to:

$$\begin{aligned} p(y_{iS}) &= \int \int p(y_{iS} | \mu_i, \lambda_i) p(\lambda_i) p(\mu_i) d\lambda_i d\mu_i \\ &= \frac{\Gamma(y_{iS} + \alpha)}{\Gamma(\alpha)y_{iS}!} \left(\frac{\beta}{\beta + E}\right)^\alpha \left(\frac{E}{\beta + E}\right)^{y_{iS}} \times W \end{aligned}$$

with

$$W = \sum_{m=1}^M \left[w_m \cdot \frac{\Gamma(a_m + b_m)\Gamma(y_{iS} + a_m)}{\Gamma(a_m)\Gamma(y_{iS} + a_m + b_m)} \times {}_2F_1 \left(y_{iS} + \alpha, b_m; y_{iS} + a_m + b_m; \frac{E}{\beta + E} \right) \right]. \quad (7)$$

Dirac-beta-Dirac distribution for the methylation level

If we consider instead of a mixture beta distribution, the DBD prior as given in Equation (4), we get the following marginal distribution:

$$p(y_{iS}, y_{iC}) = \frac{\Gamma(y_{iS} + y_{iC} + \alpha)}{\Gamma(\alpha)y_{iS}!y_{iC}!} \left(\frac{\beta}{\beta + 1 + E}\right)^\alpha \left(\frac{E}{\beta + 1 + E}\right)^{y_{iS}} \left(\frac{1}{\beta + 1 + E}\right)^{y_{iC}} \times W$$

with

$$W = w_2 + w_1 \cdot \frac{\Gamma(a + b)\Gamma(y_{iS} + a)}{\Gamma(a)\Gamma(y_{iS} + a + b)} \times {}_2F_1 \left(y_{iS} + y_{iC} + \alpha, b; y_{iS} + a + b; \frac{E}{\beta + E + 1} \right).$$

Ignoring the SssI information this marginal distribution changes to:

$$p(y_{iS}) = \frac{\Gamma(y_{iS} + \alpha)}{\Gamma(\alpha)y_{iS}!} \left(\frac{\beta}{\beta + E}\right)^\alpha \left(\frac{E}{\beta + E}\right)^{y_{iS}} \times W$$

with

$$W = w_2 + w_1 \cdot \frac{\Gamma(a + b)\Gamma(y_{iS} + a)}{\Gamma(a)\Gamma(y_{iS} + a + b)} \times {}_2F_1 \left(y_{iS} + \alpha, b; y_{iS} + a + b; \frac{E}{\beta + E} \right).$$

Parameter estimation

Independent of the prior choice for μ_i , we have to determine parameters α and β of the gamma prior distribution for λ . The default BayMeth assumes a uniform prior for μ_i , i.e. $M = 1$ and $\mu_i \sim \text{Be}(a = 1, b = 1)$, and that SssI information is taken into account, therefore α and β are the only parameters to determine. Under the empirical Bayes approach, the parameters α and β of Equation (2) can be estimated using maximum likelihood. The parameters are thereby determined in a CpG-density-dependent manner. Each 100bp bin is classified based on its CpG-density into one of $K = 100$ non-overlapping CpG-density classes: $\mathcal{C}_1, \dots, \mathcal{C}_K$. The class size $|\mathcal{C}_k|$, i.e. the number of 100bp bins in class k , is denoted by n_k . We derive for each class separately the set of prior parameters using empirical Bayes leading finally to K parameter sets. The corresponding log likelihood function for class k is then given by

$$l(\alpha^{(k)}, \beta^{(k)} | \mathbf{y}_1^{(k)}, \mathbf{y}_2^{(k)}) = \sum_{j=1}^{n_k} \log(p(y_{j1}^{(k)}, y_{j2}^{(k)} | \alpha^{(k)}, \beta^{(k)}). \quad (8)$$

Here $\mathbf{y}_S^{(k)} = (y_{1S}^{(k)}, \dots, y_{n_k S}^{(k)})$ and $\mathbf{y}_C^{(k)} = (y_{1C}^{(k)}, \dots, y_{n_k C}^{(k)})$ denote the read counts of the bins contained in class \mathcal{C}_k . Further $\alpha^{(k)}, \beta^{(k)}$ denote the parameters for CpG-density class k . In Equation (8), we assume that genomic regions are independent. For a discussion of this assumption, see the Discussion Section of the main paper. Considering a different prior distribution for μ_i the empirical Bayes approach extends to the additional parameters appearing in the prior. They will be also estimated in a CpG dependent manner. However, one should avoid including too many parameters as this complicates the empirical Bayes procedure and makes it more difficult to find the best parameters. In the case of the DBD prior distribution we fixed the weights to $w_0 = 0.1, w_1 = 0.8, w_2 = 0.1$ and only estimated the parameters a and b .

Derivation of the posterior marginal distribution Using a beta mixture prior for the methylation level

Our main interest lies in the marginal posterior distribution of the methylation level μ_i

$$p(\mu_i | y_{iS}, y_{iC}) = \int_0^{\infty} p(\lambda_i, \mu_i | y_{iS}, y_{iC}) d\lambda_i,$$

where

$$\begin{aligned}
p(\lambda_i, \mu_i | y_{iS}, y_{iC}) &= \frac{p(y_{iS}, y_{iC} | \lambda_i, \mu_i) p(\lambda_i, \mu_i)}{p(y_{iS}, y_{iC})} \\
&\stackrel{\text{cond.indep}}{=} \frac{p(y_{iS} | \lambda_i, \mu_i) p(y_{iC} | \lambda_i) p(\lambda_i) p(\mu_i)}{p(y_{iS}, y_{iC})} \\
&= \frac{\lambda_i^{y_{iS} + y_{iC} + \alpha - 1} \exp(-(E\mu_i + 1 + \beta)\lambda_i) (\beta + 1 + E)^{\alpha + y_{iS} + y_{iC}} p(\mu_i) \mu_i^{y_{iS}}}{\Gamma(y_{iS} + y_{iC} + \alpha) \times W}.
\end{aligned}$$

Here, W is as given in Equation (7), and α and β are the parameters for the gamma prior distribution for λ_i as determined by empirical Bayes (see above) for the CpG-density class to which bin i belongs.

Thus:

$$\begin{aligned}
p(\mu_i | y_{iS}, y_{iC}) &= \frac{\mu_i^{y_{iS}} p(\mu_i) (\beta + 1 + E)^{\alpha + y_{iS} + y_{iC}}}{\Gamma(y_{iS} + y_{iC} + \alpha) \times W} \int_0^\infty \lambda_i^{y_{iS} + y_{iC} + \alpha - 1} \exp(-(E\mu_i + 1 + \beta)\lambda_i) d\lambda_i \\
&= \frac{\mu_i^{y_{iS}} p(\mu_i)}{W} \left(1 - \frac{E(1 - \mu_i)}{\beta + 1 + E}\right)^{-(\alpha + y_{iS} + y_{iC})}.
\end{aligned}$$

The mean of the marginal posterior of μ_i is given by:

$$E(\mu_i | y_{iS}, y_{iC}) = \frac{A}{W}$$

with

$$A = \sum_{m=1}^M \left[w_m \cdot \frac{\Gamma(a_m + b_m) \Gamma(y_{iS} + a_m + 1)}{\Gamma(a_m) \Gamma(y_{iS} + a_m + b_m + 1)} \times {}_2F_1 \left(y_{iS} + y_{iC} + \alpha, b_m; y_{iS} + a_m + b_m + 1; \frac{E}{\beta + 1 + E} \right) \right].$$

Proof.

$$\begin{aligned}
E(\mu_i | y_{iS}, y_{iC}) &= \int_0^1 \mu_i p(\mu_i | y_{iS}, y_{iC}) d\mu_i \\
&= \frac{1}{W} \sum_{m=1}^M \left[\int_0^1 \frac{w_m \frac{\Gamma(a_m + b_m)}{\Gamma(a_m) \Gamma(b_m)} \mu_i^{a_m + y_{iS}} (1 - \mu_i)^{b_m - 1}}{\left(1 - \frac{E(1 - \mu_i)}{\beta + 1 + E}\right)^{\alpha + y_{iS} + y_{iC}}} d\mu_i \right],
\end{aligned}$$

where each integral can again be written in terms of the Gauss hypergeometric function:

$$\begin{aligned}
&\int_0^1 \frac{w_m \frac{\Gamma(a_m + b_m)}{\Gamma(a_m) \Gamma(b_m)} \mu_i^{a_m + y_{iS}} (1 - \mu_i)^{b_m - 1}}{\left(1 - \frac{E(1 - \mu_i)}{\beta + 1 + E}\right)^{\alpha + y_{iS} + y_{iC}}} d\mu_i \\
&= \frac{w_m \Gamma(a_m + b_m)}{\Gamma(a_m) \Gamma(b_m)} \int_0^1 \frac{(1 - t_i)^{a_m + y_{iS}} t_i^{b_m - 1}}{\left(1 - \frac{E}{\beta + 1 + E} t_i\right)^{\alpha + y_{iS} + y_{iC}}} dt_i \\
&= \frac{w_m \Gamma(a_m + b_m)}{\Gamma(a_m) \Gamma(b_m)} \frac{\Gamma(b_m) \Gamma(y_{iS} + a_m + 1)}{\Gamma(y_{iS} + a_m + b_m + 1)} {}_2F_1 \left(y_{iS} + y_{iC} + \alpha, b_m; y_{iS} + a_m + b_m + 1; \frac{E}{\beta + 1 + E} \right) \\
&= \frac{w_m \Gamma(a_m + b_m) \Gamma(y_{iS} + a_m + 1)}{\Gamma(a_m) \Gamma(y_{iS} + a_m + b_m + 1)} {}_2F_1 \left(y_{iS} + y_{iC} + \alpha, b_m; y_{iS} + a_m + b_m + 1; \frac{E}{\beta + 1 + E} \right).
\end{aligned}$$

□

The variance of the marginal posterior distribution of μ_i can be computed using the computational formula for the variance $\text{Var}(\mu_i|y_{iS}, y_{iC}) = \mathbb{E}(\mu_i^2|y_{iS}, y_{iC}) - (\mathbb{E}(\mu_i|y_{iS}, y_{iC}))^2$, where

$$\mathbb{E}(\mu_i^2|y_{iS}, y_{iC}) = \frac{B}{W}$$

with

$$B = \sum_{m=1}^M \left[w_m \cdot \frac{\Gamma(a_m + b_m)\Gamma(y_{iS} + a_m + 2)}{\Gamma(a_m)\Gamma(y_{iS} + a_m + b_m + 2)} \times {}_2F_1 \left(y_{iS} + y_{iC} + \alpha, b_m; y_{iS} + a_m + b_m + 2; \frac{E}{\beta + 1 + E} \right) \right],$$

so that

$$\text{Var}(\mu_i|y_{iS}, y_{iC}) = \frac{B}{W} - \left(\frac{A}{W} \right)^2.$$

Running BayMeth without a fully methylated control sample, we get

$$\mathbb{E}(\mu_i|y_{iS}) = \frac{A}{W} \quad \text{Var}(\mu_i|y_{iS}) = \frac{B}{W} - \left(\frac{A}{W} \right)^2.$$

A , B and W are:

$$\begin{aligned} A &= \sum_{m=1}^M \left[w_m \cdot \frac{\Gamma(a_m + b_m)\Gamma(y_{iS} + a_m + 1)}{\Gamma(a_m)\Gamma(y_{iS} + a_m + b_m + 1)} \times {}_2F_1 \left(y_{iS} + \alpha, b_m; y_{iS} + a_m + b_m + 1; \frac{E}{\beta + E} \right) \right], \\ B &= \sum_{m=1}^M \left[w_m \cdot \frac{\Gamma(a_m + b_m)\Gamma(y_{iS} + a_m + 2)}{\Gamma(a_m)\Gamma(y_{iS} + a_m + b_m + 2)} \times {}_2F_1 \left(y_{iS} + \alpha, b_m; y_{iS} + a_m + b_m + 2; \frac{E}{\beta + E} \right) \right], \\ W &= \sum_{m=1}^M \left[w_m \cdot \frac{\Gamma(a_m + b_m)\Gamma(y_{iS} + a_m)}{\Gamma(a_m)\Gamma(y_{iS} + a_m + b_m)} \times {}_2F_1 \left(y_{iS} + \alpha, b_m; y_{iS} + a_m + b_m; \frac{E}{\beta + E} \right) \right]. \end{aligned}$$

Using a DBD prior for the methylation level

The posterior mean and variance can be derived analogously to the previous section. Borrowing strength from a SssI sample, posterior mean and variance are given by:

$$\begin{aligned} \mathbb{E}(\mu_i|y_{iS}, y_{iC}) &= \frac{A}{W} \\ \text{Var}(\mu_i|y_{iS}, y_{iC}) &= \frac{B}{W} - \left(\frac{A}{W} \right)^2. \end{aligned}$$

with

$$\begin{aligned}
A &= w_2 + w_1 \cdot \frac{\Gamma(a+b)\Gamma(y_{iS}+a+1)}{\Gamma(a)\Gamma(y_{iS}+a+b+1)} \times {}_2F_1\left(y_{iS}+y_{iC}+\alpha, b; y_{iS}+a+b+1; \frac{E}{\beta+E+1}\right), \\
B &= w_2 + w_1 \cdot \frac{\Gamma(a+b)\Gamma(y_{iS}+a+2)}{\Gamma(a)\Gamma(y_{iS}+a+b+2)} \times {}_2F_1\left(y_{iS}+y_{iC}+\alpha, b; y_{iS}+a+b+2; \frac{E}{\beta+E+1}\right), \\
W &= w_2 + w_1 \cdot \frac{\Gamma(a+b)\Gamma(y_{iS}+a)}{\Gamma(a)\Gamma(y_{iS}+a+b)} \times {}_2F_1\left(y_{iS}+y_{iC}+\alpha, b; y_{iS}+a+b; \frac{E}{\beta+E+1}\right).
\end{aligned}$$

Assuming that no SssI sample is available, then

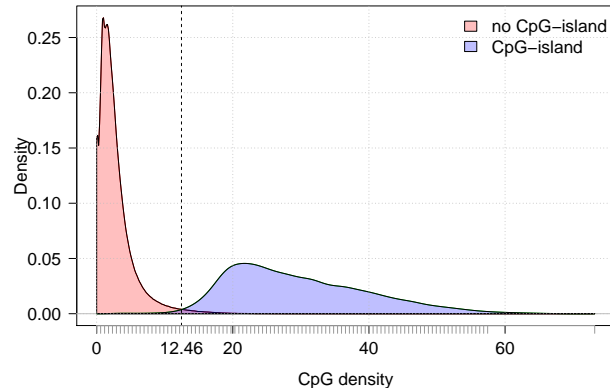
$$\begin{aligned}
\mathbb{E}(\mu_i|y_{iS}) &= \frac{A}{W} \\
\text{Var}(\mu_i|y_{iS}) &= \frac{B}{W} - \left(\frac{A}{W}\right)^2.
\end{aligned}$$

with

$$\begin{aligned}
A &= w_2 + w_1 \cdot \frac{\Gamma(a+b)\Gamma(y_{iS}+a+1)}{\Gamma(a)\Gamma(y_{iS}+a+b+1)} \times {}_2F_1\left(y_{iS}+\alpha, b; y_{iS}+a+b+1; \frac{E}{\beta+E}\right), \\
B &= w_2 + w_1 \cdot \frac{\Gamma(a+b)\Gamma(y_{iS}+a+2)}{\Gamma(a)\Gamma(y_{iS}+a+b+2)} \times {}_2F_1\left(y_{iS}+\alpha, b; y_{iS}+a+b+2; \frac{E}{\beta+E}\right), \\
W &= w_2 + w_1 \cdot \frac{\Gamma(a+b)\Gamma(y_{iS}+a)}{\Gamma(a)\Gamma(y_{iS}+a+b)} \times {}_2F_1\left(y_{iS}+\alpha, b; y_{iS}+a+b; \frac{E}{\beta+E}\right).
\end{aligned}$$

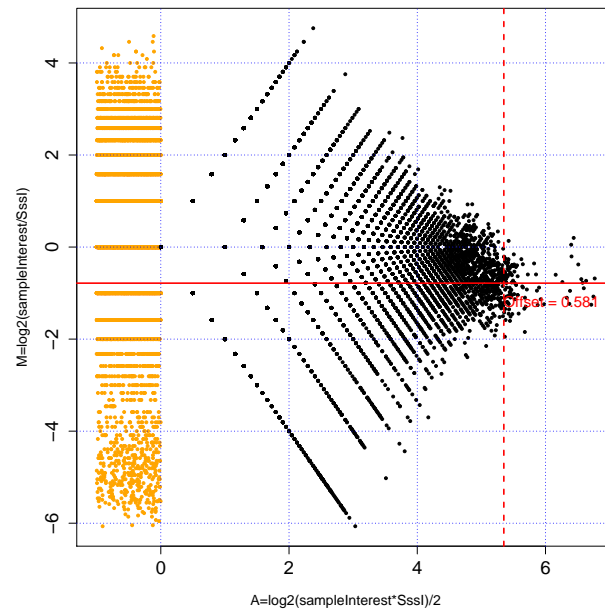
Supplementary Figures

Figure S1 - CpG-density stratified by CpG island status



Genome-wide CpG-density for bins with a mappability larger than 75% stratified by CpG island status as extracted from the `cpgIslandExt`-table of the UCSC genome browser. The vertical line marks the intersection of both densities. The grey tick-marks along the x-axis illustrate the CpG-density classes used for the empirical Bayes approach in the IMR-90 application.

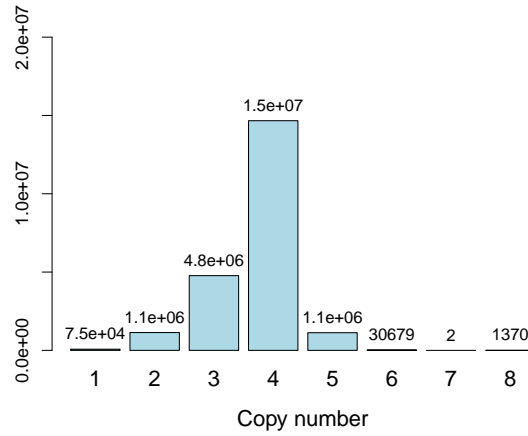
Figure S2 - Normalizing offset



Log-fold change (M) versus log-concentration (A) illustrated for 50000 randomly chosen bins. The red dotted line shows the 0.998 quantile q of A determined from all bins. The red straight line shows the estimated normalization offset $f = 2^{\text{median}(M_{A>q})}$. A 'smear' of yellow points at a low A value represents

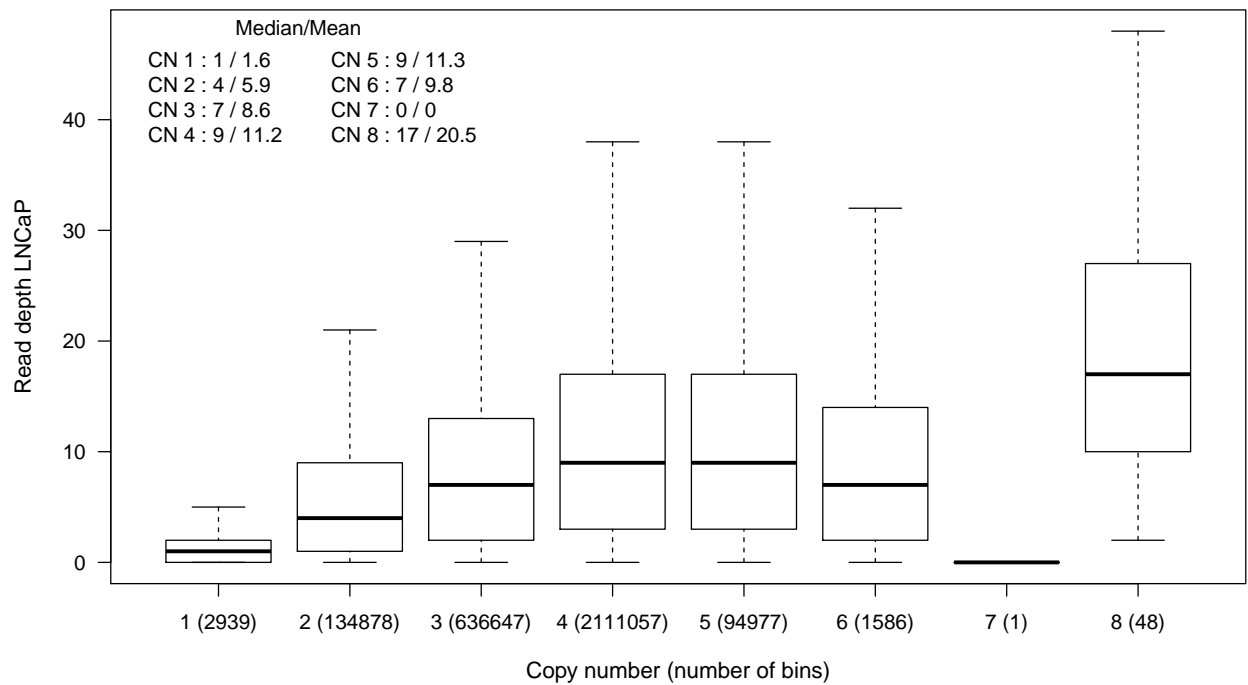
counts that are low in either of the two samples.

Figure S3 - Copy number frequencies for LNCaP



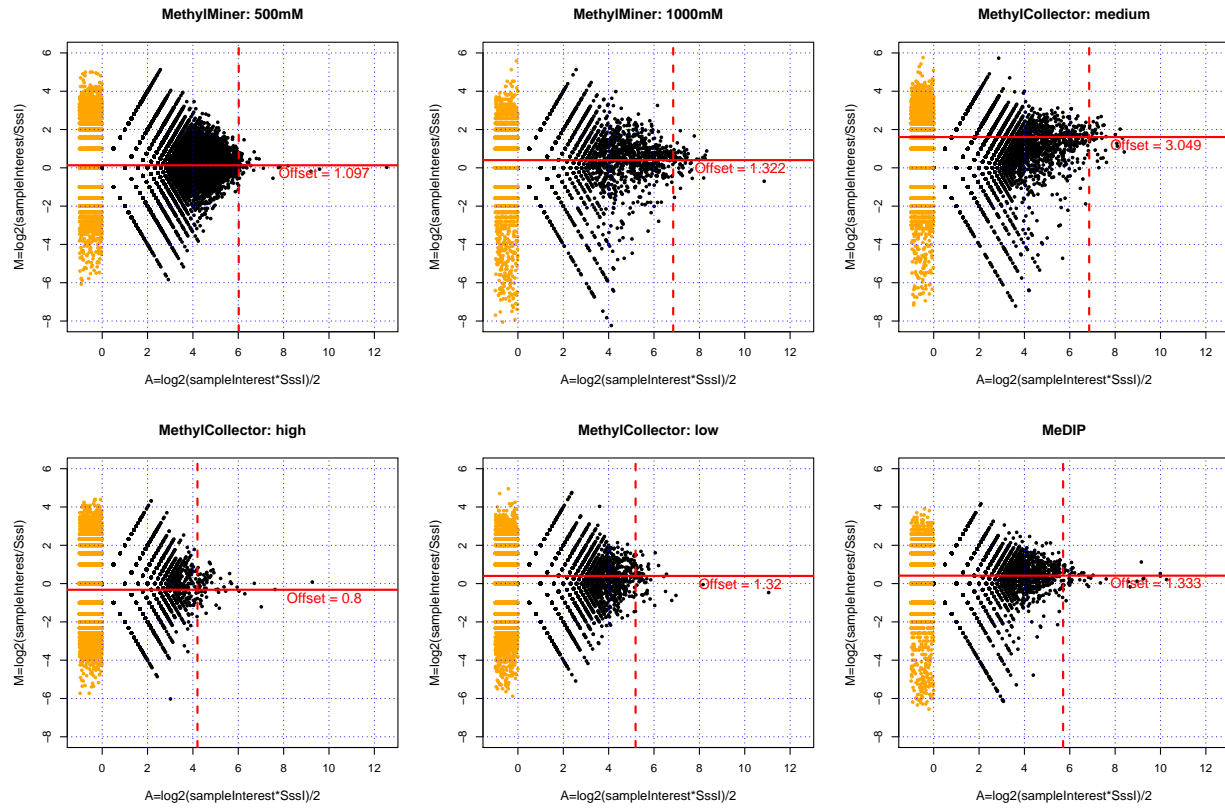
Copy number frequencies in LNCaP for 100bp-bins with a mappability larger than 0.75.

Figure S4 - Read depth of LNCaP MBD-seq by copy number



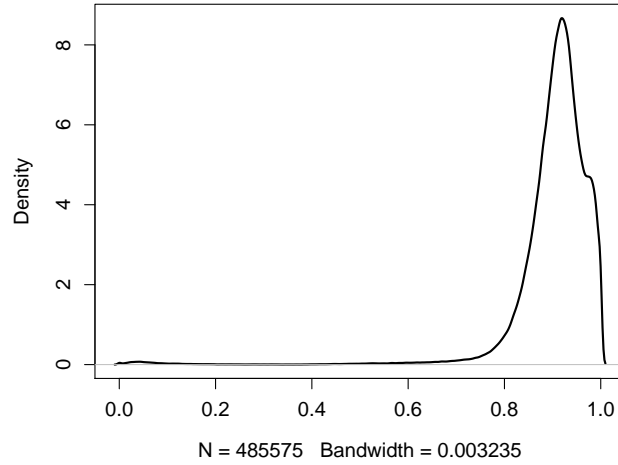
Read depth stratified by copy number is shown for 100bp-bins with a mappability larger than 0.75 and with a SssI depth larger than four. Median and mean read depth are given per copy number state.

Figure S5 - Varying normalizing offsets between methylation kits



Log-fold change (M) versus log-concentration (A) illustrated for 25000 randomly chosen bins for IMR-90 data derived using different methylation kits. The red dotted line shows the 0.998 quantile q of A determined from all bins. The red straight line shows the estimated normalization offset $f = 2^{\text{median}(M_{A>q})}$. A 'smear' of yellow points at a low A value represents counts that are low in either of the two samples.

Figure S6 - Distribution of estimated methylation levels for Sssl sample using Illumina HumanMethylation450 arrays



Density plot of 450k beta values.

Supplementary Table

Table S1 - Mean bias stratified by CpG island status and true methylation level

Method	No CpG-islands			CpG-islands		
	[0, 0.2]	(0.2, 0.8]	(0.8, 1]	[0, 0.2]	(0.2, 0.8]	(0.8, 1]
BayMeth	0.41	0.06	-0.22	0.09	0.14	-0.07
Batman	0.69	0.29	-0.01	0.11	0.15	-0.02
MEDIPS	0.05	-0.27	-0.54	0.05	-0.16	-0.47
BALM	-0.03	-0.37	-0.57	-0.01	-0.16	-0.31

Additional file 3 — BayMeth analysis of “Bock” data

We applied (default) BayMeth to the MethylCap sequencing data of [32], provided at <http://www.broadinstitute.org/labs/meissner/mirror/papers/meth-benchmark/index.html>, and denoted as the “Bock” data below. Absolute read densities are available for four samples: HUES6 ES cell line, HUES8 ES cell line, colon tumor tissue, colon normal tissue (same donor as for colon tumor tissue), based on hg18 and given for (non-overlapping) 50bp bins. There is no matched SssI sample available for these data. To take advantage of BayMeth in analyzing these data, we use a non-matching SssI sample, but one chosen to be maximally compatible to the preparation conditions of Bock data [32] (i.e. MethylCap at low salt concentration: 200mM NaCl). Furthermore, RRBS data are available for each sample representing absolute DNA methylation levels at single CpGs.

In section 1, we outline all data preparation steps. First, all samples of interest are saved in a single GRanges object based on genome-wide non-overlapping 50bp bins. RRBS information is loaded and saved in the same object. Since the read density for the fully methylated sample is based on hg19, the Bock data are lifted over. Based on hg19 we derive CpG density and mappability estimates. Finally, all information is stored in a BayMethList data object. Section 2 describes the BayMeth analysis applied on the former created BayMethList data object. Normalizing offsets are derived for all samples, before the empirical Bayes approach is used to get suitable prior parameters. Finally region-specific methylation estimates are computed.

Data preparation

Samples of interest

We applied BayMeth to the MethylCap sequencing data of [32]. Data are available for four samples: 1) HUES6 ES cell line, 2) HUES8 ES cell line, 3) Colon tumor tissue, 4) Colon normal tissue (same donor as (3)). Absolute read densities provided as bigwig files were downloaded, converted to GRanges objects and saved in a GRangesList:

	HUES6	HUES8	Colon_normal	Colon_tumor
Min.	0.00	0.00	0.00	0.00
1st Qu.	0.00	0.00	0.00	0.00
Median	0.00	0.00	0.00	0.00
Mean	2.00	1.81	1.96	1.99
3rd Qu.	2.00	2.00	2.00	2.00
Max.	374.00	400.00	407.00	400.00

Table 1: Summary information for absolute read counts for each sample.

```

setwd("./4_bock/")
library(rtracklayer)
data_names <- c("HUES6", "HUES8", "Colon_normal", "Colon_tumor")
grl_bock_methylCap <- GRangesList()
for(i in 1:length(data_names)){
  print(data_names[i])
  # import the data and convert to GRanges
  data_tmp <- import(paste("data/ChIP_absReadFreqW50_MethylCap-", data_names[i], "_all.bw", sep=""), "bw")
  data_tmp <- as(data_tmp, "GRanges")
  grl_bock_methylCap <- c(grl_bock_methylCap, GRangesList(data_tmp))
}

```

Read densities are based on (non-overlapping) 50bp bins. Summary information for each sample is shown in Table 1.

```

sumTab <- cbind(summary(values(grl_bock_methylCap[[1]])$score),
summary(values(grl_bock_methylCap[[2]])$score),
summary(values(grl_bock_methylCap[[3]])$score),
summary(values(grl_bock_methylCap[[4]])$score))

```

Of note, read density information for the different samples is not given for the same bins. To save all data in one `GRanges` object, a genome-wide `GRanges` object for hg18 based on non-overlapping 50bp was created.

```

library(BSgenome.Hsapiens.UCSC.hg18)
library(Repitools)
library(GenomicRanges)
# save all datasets in one GRanges object
gb_hg18 <- genomeBlocks(Hsapiens, 1:24, width=50)
#
tumor <- normal <- hues6 <- hues8 <- rep(NA, length(gb_hg18))
#
fo_hues6 <- findOverlaps(gb_hg18, grl_bock_methylCap[[1]])
fo_hues8 <- findOverlaps(gb_hg18, grl_bock_methylCap[[2]])
fo_normal <- findOverlaps(gb_hg18, grl_bock_methylCap[[3]])
fo_tumor <- findOverlaps(gb_hg18, grl_bock_methylCap[[4]])
#
inds_hues6 <- split(fo_hues6@subjectHits, fo_hues6@queryHits)
ind_hues6 <- as.integer(names(inds_hues6))
hues6[ind_hues6] <- values(grl_bock_methylCap[[1]])$score[fo_hues6@subjectHits]
#
inds_hues8 <- split(fo_hues8@subjectHits, fo_hues8@queryHits)
ind_hues8 <- as.integer(names(inds_hues8))
hues8[ind_hues8] <- values(grl_bock_methylCap[[2]])$score[fo_hues8@subjectHits]
#
# ... analogously for normal and tumor

df <- DataFrame("hues6"=hues6, "hues8"=hues8, "normal"=normal, "tumor"=tumor)
values(gb_hg18) <- df

```

To do this properly we have to ensure that the bins of [32] start at 1, 51, 101, 151, ... and have a width of 50bp. We have proved this using a modulo operation `table(start(grl_bock_methylCap[[i]]) %% 50)` which resulted in 1 for all bins, and `table(width(grl_bock_methylCap[[i]]))`, which resulted in 50 for all bins. Using the function `findOverlaps` the different read counts are saved as metadata at the corresponding positions in the object `gb_hg18`. If no information is provided for a bin, the read density is set to NA.

Reduced representation bisulphite sequencing (RRBS) information

Information on RRBS data are available on

<http://www.broadinstitute.org/labs/meissner/mirror/papers/meth-benchmark/RRBS/>, and used as gold standard in the following analysis. In the RRBS data for HUES6 and HUES8 we removed lines where the strand information is neither "+" , "-" nor "*", but "b", and saved the data in

RRBS_cpgMethylation_HUES6_strandCleaned.RRBS.bed and

RRBS_cpgMethylation_HUES8_strandCleaned.RRBS.bed, respectively.

Both, the number of reads that overlay a cytosine (T) and the number of cytosines that stay a cytosine (M), i.e. are methylated, are given. Note, that for one CpG site there is only information from one strand available.

```

data_names <- c("HUES6_strandCleaned", "HUES8_strandCleaned", "Colon_normal", "Colon_tumor")
# create container to save datasets
grl_bock_rrbs <- GRangesList()
for(i in 1:length(data_names)){
  # import the data and convert to GRanges
  data_tmp <- import(paste("data/RRBS_cpgMethylation_", data_names[i], ".RRBS.bed", sep=""), "BED")
  data_tmp <- as(data_tmp, "GRanges")

  # extract the number of reads that overlay a cytosine and the number
  # of cytosines that stay a cytosine i.e. are methylated
  name <- values(data_tmp)$name
  cpg <- strsplit(name, "/")
  cpg <- do.call(rbind, cpg)
  cpg <- sapply(1:ncol(cpg), function(u){as.numeric(cpg[,u])})
  colnames(cpg) <- c("numMeth", "total")

  # add the corresponding columns to the GRanges object
  # (meth correponds approximately to score/1000)
  values(data_tmp) <- cbind(values(data_tmp),
                            DataFrame(cpg, meth=cpg[,1]/cpg[,2]))

  grl_bock_rrbs <- c(grl_bock_rrbs, GRangesList(data_tmp))
}
names(grl_bock_rrbs) <- c("HUES6", "HUES8", "Colon_normal", "Colon_tumor")

```

To get smooth methylation estimates, we summarized CpG based RRBS data within 150bp bins (overlapping by 100bp). The methylation level for one 150bp bin i is thereby derived as:

$$m_i = \frac{\sum M_{\in i}}{\sum T_{\in i}}.$$

That means using information for all CpG sites that fall into bin i .


```

gb_hg18_150 <- resize(gb_hg18, 150, fix="center")
# get the corresponding rrbs estimates
meth_names <- c("rrbs_hues6_meth", "rrbs_hues8_meth", "rrbs_normal_meth", "rrbs_tumor_meth")
denom_names <- c("rrbs_hues6_denom", "rrbs_hues8_denom", "rrbs_normal_denom", "rrbs_tumor_denom")
for(i in 1:4){
  rrbs_tmp <- grl_bock_rrbs[[i]]
  fo_tmp <- findOverlaps(gb_hg18_150, rrbs_tmp)
  inds_tmp <- split(fo_tmp@subjectHits, fo_tmp@queryHits)

  nmeth <- values(rrbs_tmp)$numMeth
  total <- values(rrbs_tmp)$total

  methI <- sapply(inds_tmp, function(u) sum(nmeth[u])/sum(total[u]))
  denomI <- sapply(inds_tmp, function(u) sum(total[u]))

  denom <- meth <- rep(NA, length(gb_hg18))
  # assign the derived estimates to the corresponding genomic bins
  ind_tmp <- as.integer(names(inds_tmp))
  meth[ind_tmp] <- methI
  denom[ind_tmp] <- denomI
  tmp_df <- DataFrame(meth, denom)
  colnames(tmp_df) <- c(meth_names[i], denom_names[i])
  values(gb_hg18) <- cbind(values(gb_hg18), tmp_df)
}

```

Figure 1 shows a smooth density representation of the RRBS methylation estimates versus the MethylCap read density after filtering bins where no truth exists and only taking a minimum depth of 20 in RRBS.

Lift-over to hg19

Since the data for the fully methylated (SssI treated) sample are based on hg19, the bin coordinates of hg18 are transferred to the corresponding position on hg19.

```

chain <- import.chain("data/hg18ToHg19.over.chain")
gb_hg19 <- liftOver(gb_hg18, chain)
gb_hg19 <- unlist(gb_hg19)

```

We remove all bins with a width unequal to 50bp.

```

library(BSgenome.Hsapiens.UCSC.hg19)
w.idx <- which(width(gb_hg19) != 50)
gb_hg19r <- gb_hg19[-w.idx]

```

Lifting the bins over to hg19 caused overlapping bins. Hence, we remove all bins that have more than one overlap (namely with itself).

```

fo <- findOverlaps(gb_hg19r, gb_hg19r)
inds <- split(fo@subjectHits, fo@queryHits)
len <- unlist(lapply(inds, length))
w2.idx <- which(len != 1)
gb_hg19r <- gb_hg19r[-w2.idx]

```

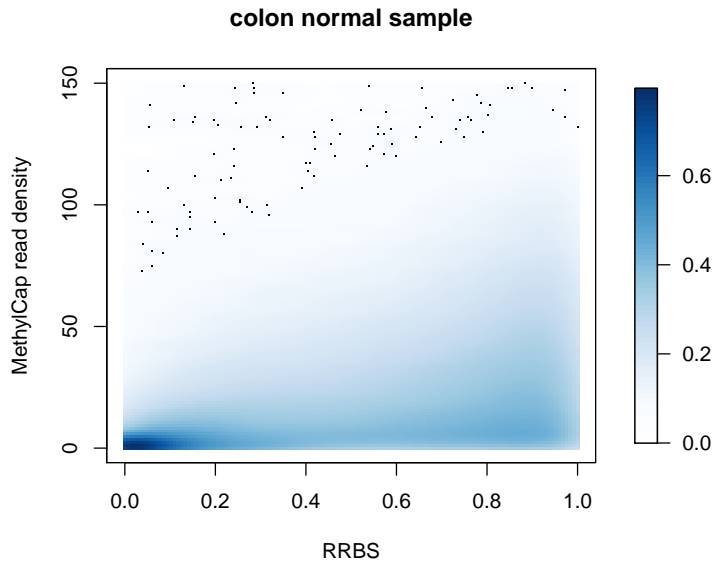


Figure 1: Comparison between read frequencies and DNA methylation levels derived from RRBS for the colon normal sample. Unprocessed read frequencies for MethylCap were correlated with DNA methylation levels as determined by RRBS.

SssI sample, CpG density and mappability information

BayMeth quantifies methylation of an affinity-enrichment sequencing dataset best by taking advantage of a full methylated control data set. Here, we use a sample treated with SssI and analysed using MethylCap at low salt concentration, i.e., 200 mM NaCl, to be maximally compatible to the preparation conditions of [32].

```
library(BSgenome.Hsapiens.UCSC.hg19)
f <- "data/SSS1_low.bam"
names(f) <- "SssI_low"
counts <- annotationBlocksCounts(f, gb_hg19r, seq.len=150)
```

The CpG density is calculated by symmetrically extending the bins around the bin center to a length of 700bp and linear weighting the CpG sites falling into this range.

```
gbA <- resize(gb_hg19r, 1, fix="center")
cpgdens <- cpgDensityCalc(gbA, organism=Hsapiens, w.function="linear", window=700)
```

Mappability probabilities are derived from <http://hgdownload.cse.ucsc.edu/goldenPath/hg19/encodeDCC/wgEncodeMapability/wgEncodeCrgMapabilityAlign50mer.bigWig>.

```

library(rtracklayer)
bw <- BigWigFile("data/wgEncodeCrgMapabilityAlign50mer_hg19.bigWig")
map <- import(bw)
score <- score(map)
wd <- width(map)
fo <- findOverlaps.gb_hg19r, map)
ind <- split(fo@subjectHits,fo@queryHits)
mapv <- numeric(length.gb_hg19r)) # default of 0
w <- as.numeric(names(ind))
# take weighted mean
mapv[w] <- sapply(ind, function(u) sum( wd[u]*score[u] ) / sum(wd[u]) )
values.gb_hg19r) <- cbind(values.gb_hg19r), DataFrame("cpgdens"=cpgdens, "map_ucsc"=mapv, "SssI-low"=counts))
save.gb_hg19r, file="data/bock_data_prepared.Rdata")

```

SssI read densities, CpG density and mappability are saved as further metadata columns in gb_h19r.

BayMeth Analysis

Here, my session info:

```
sessionInfo()
#R Under development (unstable) (2013-07-03 r63169)
#Platform: x86_64-unknown-linux-gnu (64-bit)
#
#locale:
# [1] LC_CTYPE=en_CA.UTF-8      LC_NUMERIC=C
# [3] LC_TIME=en_US.UTF-8      LC_COLLATE=en_CA.UTF-8
# [5] LC_MONETARY=en_US.UTF-8  LC_MESSAGES=en_CA.UTF-8
# [7] LC_PAPER=en_US.UTF-8     LC_NAME=C
# [9] LC_ADDRESS=C             LC_TELEPHONE=C
#[11] LC_MEASUREMENT=en_US.UTF-8 LC_IDENTIFICATION=C
#
#attached base packages:
#[1] parallel stats graphics grDevices utils datasets methods
#[8] base
#
#other attached packages:
# [1] lattice_0.20-15          fields_6.7
# [3] spam_0.29-3              Repitools_1.7.13
# [5] BSgenome.Hsapiens.UCSC.hg18_1.3.19 BSgenome_1.29.1
# [7] Biostrings_2.29.15      rtracklayer_1.21.9
# [9] GenomicRanges_1.13.36   XVector_0.1.0
#[11] IRanges_1.19.24         BiocGenerics_0.7.4
#
#loaded via a namespace (and not attached):
# [1] bitops_1.0-6            edgeR_3.3.7             grid_3.1.0              KernSmooth_2.23-10
# [5] limma_3.17.21          RCurl_1.95-4.1         Rsamtools_1.13.29      Rsolnp_1.14
# [9] stats4_3.1.0           tools_3.1.0            truncnorm_1.0-6        XML_3.98-1.1
#[13] zlibbioc_1.7.0
```

We start the analysis by loading the data. We remove bins with zero reads in all four samples and in the control, and generate a `BayMethList` object. This object is initialized with four entries:

- **windows:** A `GRanges` object representing the genomic bins of interest.
- **control:** A matrix of read counts obtained by an affinity enrichment sequencing experiment for the fully methylated (SssI) treated sample. The number of rows must be equal to `'length(windows)'`. Each column contains the counts of one sample. The number of columns must be either one or equal to the number of columns of `'sampleInterest'`.
- **sampleInterest:** A matrix of read counts obtained by an affinity enrichment sequencing experiment for the samples of interest. The number of rows must be equal to `'length(windows)'`. Each column contains the counts of one sample.
- **cpgDens:** A numeric vector containing the CpG density for `'windows'`. The length must be equal to

```

    'length(windows)')

library(Repitools)
# load the prepared data object
load("data/bock_data_prepared.Rdata")
metDat <- as.matrix(values(gb_hg19r))
# remove bins where we have no read depth in none of the samples
rs <- rowSums(metDat[, c("hues6", "hues8", "normal", "tumor", "SssI.low.SssI_low")])
wr <- which(rs == 0)
gb_hg19_noZero <- gb_hg19r[-wr]
metDat <- metDat[-wr,]
map <- metDat[, "map_ucsc"]
sssI <- matrix(metDat[, "SssI.low.SssI_low"], ncol=1)
colnames(sssI) <- "sssI"
bockBL <- BayMethList(
  window=window(gb_hg19_noZero),
  control=sssI,
  sampleInterest=cbind(hues6=metDat[, "hues6"], hues8=metDat[, "hues8"],
    normal=metDat[, "normal"], tumor=metDat[, "tumor"]),
  cpGdens=metDat[, "cpGdens"])

```

We only include autosomes in the analysis and concentrate on bins with with at least 75% mappable bases.

```

# only consider autosomes
as.idx <- !(seqnames(windows(bockBL)) %in% c("chrX", "chrY"))
as.idx <- as.vector(as.idx)
bockBL <- bockBL[as.idx]
map <- map[as.idx]
bockBL <- bockBL[map > 0.75]

```

Next, we determine the normalizing constant for each sample. The normalizing factor f is essentially a scaling factor between highly methylated regions in the corresponding sample relative to the SssI control, see Figure 2.

```

bockBL <- determineOffset(bockBL, q=0.998, controlPlot=list(show=TRUE, mfrow=c(2,2), nsamp=100000,
  main=colnames(sampleInterest(bockBL)), ask=FALSE))
f0ffset(bockBL)
#      hues6 hues8  normal   tumor
#[1,] 2.289898  2.75 1.285714 1.272727

```

Using the empirical Bayes approach we have to be aware of bins with unusual high counts of reads. These might cause problems in the optimization routine as they can cause NA or Inf values returned by the hypergeometric function. Some of these high read counts can be explained by unannotated high copy number regions, see [42]. We mask these bins out for the empirical Bayes procedure to avoid numerical problems. However, note that we will finally obtain methylation estimates for almost all of these bins.

```

## mask suspicious regions
#wget http://eqtl.uchicago.edu/Masking/seq.cov1.ONHG19.bed.gz
library(rtracklayer)
hcRegions <- import("data/seq.cov1.ONHG19.bed", asRangedData=FALSE)
bockBL <- maskOut(bockBL, hcRegions)

```

Using this reduced dataset we derive the prior parameters based on empirical Bayes. We use a uniform

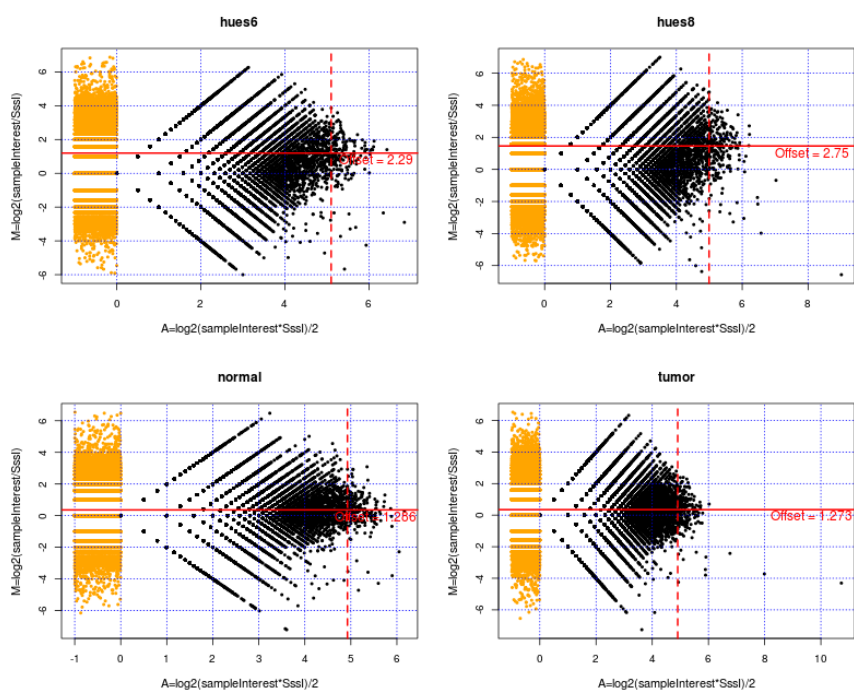


Figure 2: Log-fold change (M) versus log-concentration (A) illustrated for all four samples randomly sampling data of 100000 bins in each case. The red dotted line shows the 0.998 quantile q of A determined from all bins. The red straight line shows the estimated normalization offset $f = 2^{\text{median}(M_{A>q})}$. A 'smear' of yellow points at a low A value represents counts that are low in either of the two samples.

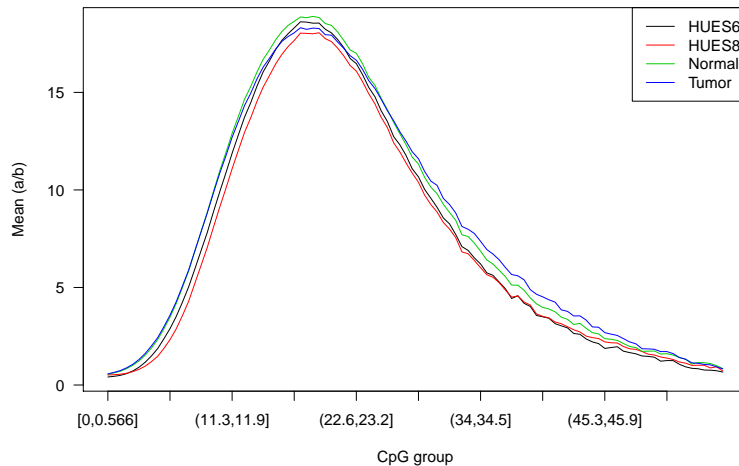


Figure 3: Mean of the prior predictive distribution depending on CpG density group for all four samples.

prior distribution for the methylation level and consider $K = 100$ separate CpG groups. The algorithm is run on four CPUs in parallel.

```
## find prior parameters using empirical Bayes
bockBL <- empBayes(bockBL, ngroups = 100, ncomp = 1, maxBins = 50000,
  method="beta", ncpu=4, verbose=FALSE)
```

The prior parameters for all samples are saved in a list, which can be accessed using the function `priorTab(.)`. The first list element contains a vector with the assigned CpG density group for each bin. Of note, the length of this vector is equal to the numbers of bins used in the analysis. The second list element saves the number of mixture components used and the third contains a string indicating the type of prior ("beta" or "DBD"). The following entries contain the prior parameters for each sample. One list element corresponds thereby to one sample. Figure 3 shows the mean of the obtained prior predictive distribution of the SssI sample depending on CpG density group for all four samples.

```
plot(priorTab(bockBL)[[4]][1,]/priorTab(bockBL)[[4]][2,],
  type="l", xlab="CpG group", ylab="Mean (a/b)", xaxt="n")
axis(1, at=seq(1,100,10), labels=levels(priorTab(bockBL)[[1]])[seq(1,100,10)])
for(i in 2:4){
  lines(priorTab(bockBL)[[3+i]][1,]/priorTab(bockBL)[2,], type="l", col=i)
}
legend("topright", c("HUES6", "HUES8", "Normal", "Tumor"), lty=1, col=1:4)
```

To get methylation estimates we call:

```
bockBL <- methylEst(bockBL, verbose=TRUE, controlCI = list(compute = FALSE))
```

This function assigns a list to the slot `methEst` in our `BayMethList` object. Here, the mean, variance and potential credible intervals are saved for each sample. The mean and variance can be accessed using

```
methEst(bockBL)$mean and methEst(bockBL)$var .
```

Figure 4 shows regional methylation estimates of BayMeth compared to RRBS for all samples.


```

mE <- methEst(bockBL)$mean
mV <- methEst(bockBL)$var
cP <- cpgDens(bockBL)
sssI <- control(bockBL)
sI <- sampleInterest(bockBL)
## get the truth for all samples
rrBS <- as.matrix(values(windows(bockBL))[,5:12])
rrBS <- as.matrix(rrBS)
#
# combine everything in one matrix to facilitate plotting
all <- cbind(mE, rrBS, cP, sssI, sI, mV)
colnames(all) <- c("bayMeth_hues6", "bayMeth_hues8", "bayMeth_normal", "bayMeth_tumor",
  colnames(rrBS), "cpgDens", "sssI", "hues6", "hues8", "normal", "tumor",
  "bayMeth_varHues6", "bayMeth_varHues8", "bayMeth_varNormal", "bayMeth_varTumor")
#
sNames <- c("a) HUES6", "b) HUES8", "c) Colon normal", "d) Colon tumor")
#
alls <- all
#
col <- "dodgerblue4"
Lab.palette <- colorRampPalette(c("blue", "orange", "red"), space = "Lab")
par(mfrow=c(2,2), mar=c(3.5,4, 3, 4.5), mgp=c(2.5,1,0), cex.lab=.85, cex.main=1, cex.axis=.75, pty="s", las=1)
zlim <- c(0,2.34)
lim <- c(0,1)
for(i in 1:4){
  all <- alls
  all <- all[!is.na(all[,5+2*(i-1)]),]
  all <- all[!is.na(all[,i]),]
  #
  ## define a limit for the truth
  limit_truth <- 20
  all <- all[all[,6+2*(i-1)] > limit_truth,]
  #
  ## separation by variance
  limit_var <- 0.0225
  all <- all[all[,19+(i-1)] < limit_var,]
  #
  ## separation by SssI control
  limit_control <- 9
  all <- all[all[,"sssI"] > limit_control,]
  #
  ## smooth density representation
  mysmoothScatter(all[,5+2*(i-1)], all[,i], pch=".",
    col=col, colramp=Lab.palette, xlab="RRBS", ylab="BayMeth",
    main=sNames[i], xlim=lim, ylim=lim,
    cex=0.05, horizontal=F, zlim=zlim,
    axis.args=list(at=zlim, labels=c("low", "high")))
  text(0.5, 0.05, sum(!is.na(all[,i])), col="white", cex=0.85)
  abline(c(0,0), c(1,1), col="green", lwd=1.3, lty=2)
}

```

Here, `mysmoothScatter` represents an adaptation of the function `smoothScatter` to get a color key next to the figures.

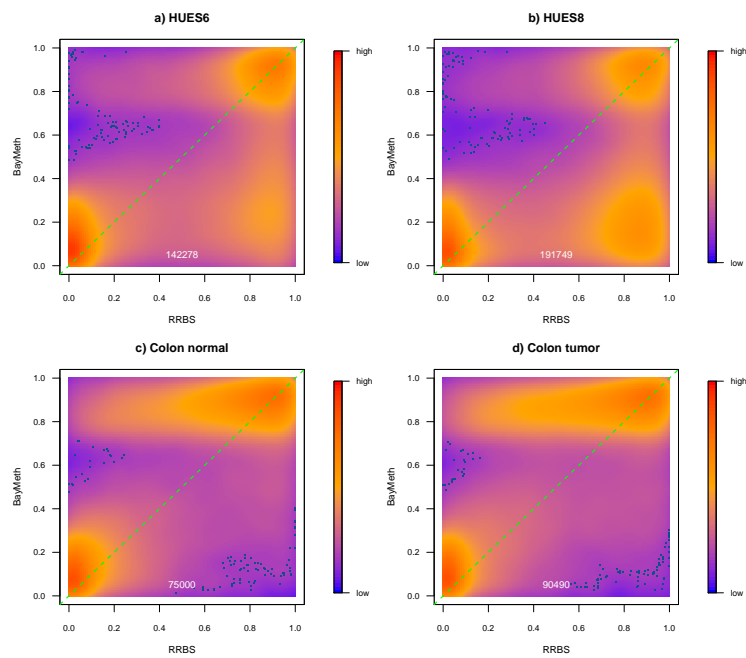


Figure 4: Smooth color density representation of variance estimates obtained by BayMeth versus number of reads in the SssI control for a read depth larger than 20 in RRBS. The red box contains the bins used in Figure 9 having at least a depth of 10 in SssI and a standard deviation smaller than 0.15, i.e. a variance smaller than 0.025.